EUROPEAN RESPIRATORY *journal*

FLAGSHIP SCIENTIFIC JOURNAL OF ERS

Early View

Original article

Topological data analysis reveals genotype-phenotype relationships in primary ciliary dyskinesia

Amelia Shoemark, Bruna Rubbo, Marie Legendre, Mahmood R. Fassad, Eric G. Haarman, Sunayna Best, Irma C.M. Bon, Joost Brandsma, Pierre-Regis Burgel, Gunnar Carlsson, Siobhan B. Carr, Mary Carroll, Matt Edwards, Estelle Escudier, Isabelle Honoré, David Hunt, Gregory Jouvion, Michel R. Loebinger, Bernard Maitre, Deborah Morris-Rosendahl, Jean-Francois Papon, Camille M. Parsons, Mitali P. Patel, N Simon Thomas, Guillaume Thouvenin, Woolf T. Walker, Robert Wilson, Claire Hogg, Hannah M. Mitchison, Jane S. Lucas

Please cite this article as: Shoemark A, Rubbo B, Legendre M, *et al*. Topological data analysis reveals genotype-phenotype relationships in primary ciliary dyskinesia. *Eur Respir J* 2021; in press (https://doi.org/10.1183/13993003.02359-2020).

Topological data analysis reveals genotype-phenotype relationships in primary ciliary dyskinesia

Shoemark, Amelia.[1,2,*], Rubbo, Bruna.[3,4,*], Legendre, Marie.[5,6], Fassad, Mahmood.R.[7,8], Haarman, Eric.G.[9], Best, Sunayna.[7,10], Bon, Irma.C.M.[9], Brandsma, Joost.[4], Burgel, Pierre-Regis.[11,12], Carlsson, Gunnar.[13], Carr, Siobhan.B.[1], Carroll, Mary.[3,4], Edwards, Matt.[14], Escudier, Estelle.[5,6], Honoré, Isabelle.[11], Hunt, David.[15], Jouvion, Gregory.[5,6], Loebinger, Michel.R.[16], Maitre, Bernard.[17,18], Morris- Rosendahl, Deborah.[14], Papon, Jean-Francois.[19,20,21,22], Parsons, Camille .M.[23], Patel, Mitali.P.[7], Thomas, N.Simon[24,25], Thouvenin, Guillaume.[26,274], Walker, Woolf .T.[3,4], Wilson, Robert.[16], Hogg, Claire.[1], Mitchison, Hannah.M.[6,28,‡], Lucas, Jane.S.[3,4,‡]

*Equal first author contribution

[1] PCD Diagnostic Centre and Department of Paediatric Respiratory Medicine, Royal Brompton and Harefield NHS Trust, London SW3 6NP, UK.
[2] Division of Molecular and Clinical Medicine, University of Dundee, Ninewells Hospital and Medical School, Dundee DD1 9SY, UK.
[3] Primary Ciliary Dyskinesia Centre, University Hospital Southampton NHS Foundation Trust, Southampton SO17 1BJ, UK.
[4] School of Clinical and Experimental Sciences, University of Southampton Faculty of Medicine, Southampton SO17 1BJ, UK

[5] Département de Génétique Médicale, Hôpital Trousseau, Assistance Publique-Hôpitaux de Paris (AP-HP), F-75012 Paris, France.
[6] Sorbonne Université, Institut National de la Santé et de la Recherche Médicale INSERM, U933, Hôpital Trousseau, F-75012 Paris, France.
[7] Genetics and Genomic Medicine Department, University College London, UCL Great Ormond Street Institute of Child Health, London WC1N 1EH, UK.
[8] Department of Human Genetics, Medical Research Institute, Alexandria University, Egypt. 165 El-Horreya Avenue, Alexandria 21561, Egypt.
[9] Department of Pediatric Pulmonology, Emma Children's Hospital, Amsterdam UMC, Vrije Universiteit Amsterdam, the Netherlands.
[10] Leeds Institute of Medical Research, Faculty of Medicine and Health, University of Leeds, Leeds, LS9 7TF, UK.
[11] Service de Pneumologie, Hôpital Cochin, Assistance Publique-Hôpitaux de Paris (AP-HP), F-75014 Paris, France.

[12] Université de Paris, Institut National de la Santé et de la Recherche Médicale INSERM, U1016, Institut Cochin, F-75014 Paris, France.
[13] Department of Mathematics, Stanford University, Stanford, California 94305, USA
[14] Clinical Genetics and Genomics, Royal Brompton and Harefield NHS Foundation Trust, London SW3 6NP, UK.
[15] Wessex Clinical Genetics Service, University Hospitals Southampton, Princess Anne Hospital, Coxford Road, Southampton SO16 5YA, UK.
[16] Host Defence Unit, Department of Respiratory Medicine, Royal Brompton and Harefield NHS Foundation Trust, London, UK. NHLI, Imperial College, London SW3 6NP, UK.
[17]Service de Pneumologie, DHU A-TVB, Centre Hospitalier Intercommunal de Créteil, Université Paris Est, F-94000 Créteil, France.
[18] Institut Mondor de Recherche Biomédicale (IMRB), Unité Inserm U955, F-94000 Créteil, France.
[19] Service d'ORL et Chirurgie Cervico-Faciale, Hôpital Kremlin-Bicêtre, Assistance Publique-Hôpitaux de Paris (AP-HP), F-94270 Le Kremlin-Bicêtre, France.
[20] Faculté de Médecine, Université Paris-Saclay, F-94070 Le Kremlin-Bicêtre, France.
[21] CNRS, ERL 7240, F-94010 Créteil, France.
[22] Institut National de la Santé et de la Recherche Médicale INSERM, U955, F-94010 Créteil, France.
[23] MRC Lifecourse Epidemiology Unit, University of Southampton, Southampton SO17 1BJ, UK.
[24] Wessex Regional Genetics Laboratory, Salisbury NHS Foundation Trust, Salisbury SP2 8BJ, UK.
[25] Human Genetics and Genomic Medicine, University of Southampton Faculty of Medicine, Southampton SO17 1BJ, UK
[26] Service de Pneumologie Pédiatrique, Hôpital Trousseau, Assistance Publique-Hôpitaux de Paris (AP-HP), F-75012 Paris, France
[27] Sorbonne Université, INSERM, Centre de Recherche Saint-Antoine, F-75012 Paris, France.
[28] NIHR Great Ormond Street Hospital Biomedical Research Centre, London WC1N 3JH, UK.

[‡]**Joint corresponding authors:**
Professor Jane Lucas, Southampton University Hospital, Mailpoint 803 F level, Tremona Road, Southampton, SO16 6YD, UK. E-mail: jlucas1@soton.ac.uk Phone: +44 238120 6160
Professor Hannah M. Mitchison, Genetics and Genomic Medicine, University College London, UCL Great Ormond Street Institute of Child Health, London WC1N 1EH, UK.
E-mail: h.michison@ucl.ac.uk. Phone: +44 207 905 2866

Running head: Genotype-phenotype in primary ciliary dyskinesia

Key words: primary ciliary dyskinesia, genotype, phenotype, cilia, diagnosis, genetic testing

Tweetable ERS abstract:

Topological data analysis of 396 primary ciliary dyskinesia patients shows genetic mutations of worse (*CCDC39*), variable (*DNAH5*) and milder (*DNAH11*) effects on lung function, offering the potential for more accurately targeted disease management.

Author contributions

Concept and design of the study: JSL, CH, HMM, AS, BR

Genotyping: HMM, MRF, MMP, SNT, DH, ME, DM-R, ML

Clinical characterisation: JSL, CH, WTW, MC, SBC, MRL, RW, EGH, J-FP, BM, GT, P-RB, IH

TDA models: BR, JB, GC

Data collection: BR, AS, SB, WTW, CH, J-FP, BM, GT, P-RB, IH, EGH, ICMB, EE, GJ, ML

Planned and performed the statistical analyses: BR, AS, CMP, JSL

Laboratory analyses and data collection: EE, GJ, AS, ML, SB, HMM, MRF

Interpretation of data analyses: BR, AS, JSL, HMM, CH

Drafted the manuscript. AS, BR, JSL, HMM, CH

Revised the manuscript. JSL, CH, HMM, AS, BR, NST, ML, MF, WTW, SBC, IH, EE

All authors have read and approved the final manuscript. HMM and JSL had full access to all data and take final responsibility for the decision to submit for publication.

Funding: The PCD Centres in Southampton and London, the Wessex Regional Genetics Laboratory and Wessex Clinical Genetics Service are funded by the National Health Service for England (NHSE). Clinical research in Southampton was supported by NIHR Southampton

Respiratory BRC and NIHR Southampton Wellcome Trust Clinical Research Facility. H.M.M. acknowledges support from Action Medical Research, Great Ormond Street Children's Charity and the NIHR Great Ormond Street Hospital Biomedical Research Centre. M.R.F was also supported by NIHR GOSH BRC and a PhD studentship from the British Council Newton-Mosharafa Fund and Ministry of Higher Education in Egypt. In France this work was supported by the Institut National de la Santé et de la Recherche Médicale (INSERM), the RaDiCo funded by the French National Research Agency under the specific programme "Investments for the Future" (Cohort grant agreement ANR-10-COHO-0003) and the Legs Poix grant from the Chancellerie des Universités of Sorbonne Universités. The funders had no role in the writing of the manuscript or the decision to submit it for publication. We have received no payment to write this article. JSL and HMM had full access to all the data in the study and had final responsibility for the decision to submit for publication.

Abstract

Background Primary ciliary dyskinesia (PCD) is a heterogeneous inherited disorder caused by mutations in approximately 50 cilia-related genes. PCD genotype-phenotype relationships have mostly arisen from small case series because existing statistical approaches to investigate relationships have been unsuitable for rare diseases.

Methods We applied a topological data analysis (TDA) approach to investigate genotype-phenotype relationships in PCD. Data from separate training and validation cohorts included 396 genetically defined individuals carrying pathogenic variants in PCD genes. To develop the TDA models, twelve clinical and diagnostic variables were included. TDA-driven hypotheses were subsequently tested using traditional statistics.

Results Disease severity at diagnosis measured by FEV_1 z-score was (i) significantly worse in individuals with *CCDC39* mutations compared to other gene mutations and (ii) better in those with *DNAH11* mutations; the latter also reported less neonatal respiratory distress. Patients without neonatal respiratory distress had better preserved FEV_1 at diagnosis. Individuals with *DNAH5* mutations were phenotypically diverse. Cilia ultrastructure and beat pattern defects correlated closely to specific causative gene groups, confirming these tests can be used to support a genetic diagnosis.

Conclusions This large scale multi-national study presents PCD as a syndrome with overlapping symptoms and variation in phenotype, according to genotype. TDA modelling confirmed genotype-phenotype relationships reported by smaller studies (e.g. FEV_1 worse with *CCDC39* mutations), and identified new relationships, including FEV_1 preservation with *DNAH11* mutations and diversity of severity with *DNAH5* mutations.

Introduction

Primary ciliary dyskinesia (PCD) is clinically and genetically heterogeneous. Symptoms relate to dysfunction of multiple motile cilia and can include neonatal respiratory distress syndrome (NRDS), wet cough, recurring upper and lower respiratory tract infections, otitis media, bronchiectasis, infertility, situs inversus and congenital heart disease (CHD) [1]. Mutations in 50 ciliary genes have been described so far [2, 3].

Understanding of genotype-phenotype relationships informs diagnostic decisions and treatment, but due to the rarity (≈1:10 000) and diversity of PCD, and the constraints of traditional statistical methods, a large patient cohort has never been studied for genotype-phenotype relationships. Evidence for clinically relevant genotype-phenotype associations is mostly limited to small case series for a specific gene or clinical characteristic. For example, individuals with variants in *HYDIN*, a radial spoke head gene, or in multiciliogenesis gene variants like *MCIDAS* and *CCNO* are unlikely to have situs inversus, as nodal cilia are not affected [4-7]. Using traditional statistical approaches, cohort studies have been underpowered to investigate by single genes, and instead have combined functionally similar genes for analysis. A North American study of 137 children reported worse lung disease in those with central apparatus or microtubular disorganisation with inner dynein arm ultrastructural defects, most of whom have *CCDC39* and *CCDC40* variants, than in patients with outer dynein arm defects caused by *DNAH5* variants [8, 9].

Topological data analysis (TDA) allows for the visual exploration of data without establishing *a priori* hypotheses [10]. It can be used to explore the underlying patterns in complex datasets by generating clusters of individuals with similar features in multiple dimensions in an unsupervised

manner, as extensively validated in several clinical studies [11-13]. TDA can be used to highlight small groups of interest in large or complex datasets, that could be overlooked when applying traditional clustering methods that are typically more constrained by a requirement for pre-selection of parameters (e.g. definition of the number of clusters) to drive data analyses [10, 14]. In doing so, TDA can uncover patient subgroups more likely to benefit from a particular therapeutic intervention [12, 15-17]. It thereby provides a promising approach to investigate genotype-phenotype associations in heterogeneous patients with rare diseases.

We aimed to investigate relationships between clinical, diagnostic and genetic data, hypothesising that different subgroups of PCD patients with particular clinical and diagnostic phenotypes could be identified according to their underlying genotypes.

Methods

Ethics

Local and national research and ethical approvals were obtained and adhered to (NRES Committee South Central Hampshire Ethics 06/Q1702/109, London Bloomsbury Research Ethics Committee 08/H0713/82 and Ile-de-France Ethics Committee CPP07729).

Study Design

Clinical and diagnostic data were retrospectively collected from patients with a confirmed genetic diagnosis of PCD i.e. carrying autosomal bi-allelic variants or an X-linked variant classified as pathogenic according to international guidelines [18, 19]. **Supplementary table E1** shows the data coding for the clinical characteristics included in the study.

The study design was based on previous TDA studies and is outlined in **figure 1** [15]. TDA was performed in order to generate hypotheses, which could be tested using more traditional statistical testing. TDA was applied to a discovery cohort of 199 patients (cohort details and genetics can be found in **supplementary tables E2, E3, E4**) and validated using a second cohort of 197 patients (cohort details and genetics can be found in **supplementary figure E1** and **tables E5, E6**). An overview of the PCD genes affected by mutations in the full study population is shown in **supplementary figure E2**.

Topological data analysis

Topological models were developed using a licensed version of TDA software through the Symphony AyasdiAI cloud-based platform (www.ayasdi.com, v 2.0, Ayasdi Inc., Menlo Park, CA). More details of TDA are in the supplementary file.

The phenotypic data used for clustering were body mass index (BMI), forced expiratory volume in 1 second (FEV_1) z-score, forced vital capacity (FVC) z-score, neonatal respiratory distress (NRDS), wet cough, rhinitis, glue ear, cardiac situs, congenital heart disease (CHD), nasal nitric oxide (nNO), ciliary beat pattern (CBP) and transmission electron microscopy (TEM). Genetic data were not used to generate the topological models, as these were the study's main variable of interest; genes of interest were later mapped onto the models to develop hypotheses regarding genotype-phenotype associations.

Models were generated using an automated analysis option. Locally linear embedding (LLE) is a non-linear dimensionality reduction technique, on which highly complex data are summarised and compressed into smaller representations of their variability. The topological model with the best-defined clusters upon visual inspection used two LLE lenses and the correlation distance as metric (i.e. distance function). These identical parameters were applied to develop the discovery and validation models.

The Mapper algorithm was used to identify coherent groups of samples [20]. Each node of the topology model constitutes patients who have combinations of features that are similar between each other, with connecting lines (edges) representing data points that are shared between nodes. The size of the node represents the number of subjects with that specific combination of features.

Genotypes were mapped onto the model to visualise hypothesised associations between genotype and phenotypic clusters. Validation of hypotheses suggested by TDA were then performed using standard statistical analysis. Generating hypotheses using TDA prevented the requirement for multiple comparisons and loss of statistical power.

TDA is an effective method to apply in clinical studies as it can allow for missing data[21]. More detailed explanation of TDA can be found in the **supplementary material**.

Statistical analysis

Selection of variables for hypothesis testing was guided by the topological models to limit the number of comparisons. Further methodological details are provided in the **supplementary material**.

The derived hypotheses were tested through statistical analyses of the whole dataset and of the validation dataset alone. Where the same outcome was tested twice, p-values were adjusted using the Bonferroni correction ($p \leq 0.049$ was found to be significant). Continuous data were compared using student t-tests, ANOVA and Kruskal-Wallis, and categorical data were compared using chi-square or Fisher's exact tests. Tukey's test was used for pairwise comparisons following ANOVA and Dunn's test with Holm-Sidak adjustment following Kruskal-Wallis.Multiple regression models were used to model FEV_1 z-scores, adjusting for age at diagnosis, history of NRDS and presence of CHD. Normality of residuals was investigated using kernel density estimations, and visual inspection of histograms and residuals versus fits graph plots. Number of observations (*n*), regression coefficients (r) with 95% confidence intervals (CI) and model's goodness-of-fitness (adjusted R^2) were reported for each model. Data were analysed in STATA (version 14.0, StataCorp, College Station, TX).

Results

Data-driven genotype-phenotype associations using topological data analysis in a discovery group of 199 PCD patients

Genotype and diagnostic test phenotype associations

TEM defect and CBP mapped visually very closely to corresponding gene group (**figure 2**).

Genotype and FEV_1 associations

Systematic exploration of each of the features collected for this study showed that patients with defects in the 'radial spoke/central complex' and 'nexin-dynein regulatory complex (N-DRC)/molecular ruler' gene functional groups had worse FEV_1 z-scores at diagnosis (as indicated in **figure 3.B** by dark blue coloured nodes) than those with dynein structural gene mutations (higher FEV_1 z-scores, indicated in white coloured nodes in **figure 3.B**). Interestingly, in the cluster with predominantly poor FEV_1 (**figure 3.B** in dark blue), which corresponds to N-DRC or molecular ruler genes (*CCDC39, CCDC40, CCDC65, DRC1;* **figure 3A**), there was a defined group showing absence of history of rhinitis (**supplementary figure E3.B).**

The group with predominantly preserved lung function at diagnosis (**figure 3.B** in white) corresponds to a cluster of individuals with absence of NRDS (**figure 3.C** in white) and an area associated with gene defects of dynein structure (**figure 3.A.** in blue). Further exploration of the topological model showed that within this dynein structural defects group, it was predominantly *DNAH11* patients that had preserved lung function at diagnosis and absence of NRDS (**figure 3.E** in green).

In contrast, individuals with variants in *DNAH5* (the commonest genetic cause of PCD and most predominant patient group in the cohort) were a phenotypically diverse group regarding lung function, with no clear cluster observed (**figure 3.F**).

Genotype and other clinical phenotype associations

The model shows a group of patients with central complex and N-DRC/molecular ruler gene mutations without situs inversus but increased likelihood of glue ear (**supplementary figures E3.A** in yellow and orange, **E3.C** in red) [7, 22]; and a lack of laterality defects associated to *MCIDAS* and *CCNO* in the 'other function' gene group (**supplementary figure E3.D**; red) [6, 23]. Conversely, TDA revealed a cluster of patients with absence of glue ear; this was a genetically diverse group of individuals with dynein structural and assembly defects (**supplementary figures E3.A** in blue and green and **E3.C** in white).

Validation using topological data analysis in a replication group of 197 PCD patients

A validation topological model was generated by analysis of a replication cohort of 197 additional patients: 61 from the UK, 28 from the Netherlands and 108 from France (**supplementary tables E5, E6**). This confirmed the discovery group findings, with *CCDC39* mutation patients clustering in an area of the structure with lower FEV_1 z-scores at diagnosis (**figure 4.B** in dark blue and **figure 4.D** in green) and a higher proportion of reported NRDS (**figure 4.C** in red), while *DNAH11* mutation patients clustered in an area with higher FEV_1 z-scores (**figure 4.E** in green and **figure 4.B** in light blue and white) and less reported NRDS (**figure 4.C** in red and white). The model also confirmed the absence of a clear cluster of patients with *DNAH5* mutations (**figure 4.F** in green). Additional features of the validation cohort are shown in **supplementary figure E4.**

When analysing gene groups, those with mutations in the 'dynein regulatory/molecular ruler' genes category had worse FEV_1 z-scores (**figure 4.A** in orange and **figure 4.B** in dark blue) and less rhinitis (data not shown) at diagnosis, as seen in the discovery model. The cluster with preserved lung function was mostly formed by patients with dynein structure gene variants (**figure 4.B** in light blue and white and **figure 4.A** in blue), particularly *DNAH11* (**figure 4.E** in green).

However, we could not confirm the inverse association between upper airway (rhinitis and glue ear) and lower airway disease (FEV_1 and NRDS) observed in the discovery model (Figure E4).

The distribution of gene variants in the total 396 patients from both cohorts, in 31 PCD genes, is shown in **figure 5** and the clinical and diagnostic characteristics in **supplementary tables E7 & E8.**

Validation of hypothesis suggested by TDA using standard statistical analysis

Two genes, *CCDC39* and *DNAH11*, fulfilled the criteria for further hypothesis-driven statistical analysis. This required the identification of clearly defined clusters of patients with mutations in each gene showing distinct features, in both the hypothesis-driving discovery (**figure 3**) and the validation (**figure 4**) topological models, along with sufficient patients in each phenotype to allow standard statistical approaches (n = 35 and 48, respectively, **figure 5**). These two genes clustered in areas with extreme values of FEV_1 z-scores in both topological models, leading to the hypothesis that *CCDC39* and *DNAH11* patients had a distinct respiratory phenotype compared to the rest of the study population.

Testing these hypotheses using traditional statistical analyses, *CCDC39* mutation patients had significantly lower FEV_1 z-scores at diagnosis compared to all other patient genotypes grouped

together (r = -1.2; 95% CI, -1.88 to -0.55, adjusted R^2 = 8.0%, p<0.001 *n* = 205), adjusted for age at diagnosis, NRDS and CHD. Conversely, those with *DNAH11* had significantly higher FEV_1 z values at diagnosis (r = 0.09; 95% CI, 0.27 to 1.53; adjusted R^2 = 5.8%, p = 0.003, *n* = 205) and reported less NRDS compared to patients with mutations in any of the other genes (41.03% vs 63.91%, p=0.008).

In contrast, there were no statistically significant differences in NRDS for patients with *CCDC39* mutations (67.86% vs 60.29% for any of the other genes), or in upper airway symptoms (i.e. rhinitis and glue ear) for patients with *CCDC39* (96.77%) or *DNAH11* mutations (97.67%) compared to any of the other genes (93.44% and 93.18%, respectively).

Discussion

This is the first large-scale study to systematically investigate associations between genotype and phenotype in the genetically heterogeneous disorder PCD. It demonstrates the use of a new methodology for the visualisation of data and generation of hypotheses complementing more traditional statistical approaches, where used alone these would not be sufficiently powered, even in multinational cohorts. TDA cluster modelling in nearly 400 individuals from three European countries identified several previously unknown genotype-phenotype relationships, in addition to confirming previously reported genetic associations [7, 22, 24]. PCD, a disease with many well-defined features and 50 causal genes, leant itself to TDA and machine learning for the identification of distinct phenotypic clusters that might share an underlying genetic mutation. TDA was able to identify clinical patterns amongst relatively small numbers of patients (<40) with mutations in a particular gene. We suggest the approach might be beneficial for similar rare diseases, where traditional statistical methods are not suitable.

The TDA model confirmed well-established associations between diagnostic tests (TEM, CBP) and genetics, as seen by the similar colour patterns in the topological models (**figure 2**) where TEM defect and CBP mapped visually very closely to corresponding gene group. This confirms a strong association that is in agreement with the published PCD literature [2, 21]. Distinct genetic findings were also associated with disease severity. We found *CCDC39* patients had significantly worse lung function at diagnosis (FEV_1 z-score) when compared to all other groups, as has previously been observed in individuals with microtubular defects [8, 9, 25, 26]. Furthermore, modelling identified other findings not reported before, including that individuals with *DNAH11* mutations were significantly less likely to have NRDS and, in turn, that the absence of NRDS is associated with better lung function at diagnosis. These findings were

consistent between discovery and validation groups, and when using traditional statistical approaches.

The underlying pattern of the discovery topological model data suggests that patients with compromised lower airways at diagnosis (i.e. decreased lung function and history of NRDS) reported less upper airway symptoms (i.e. history of glue ear and rhinitis). However, these findings could not be verified in the validation model; as they may result from over-fitting of the model, this requires independent validation in an adequately powered independent dataset.

Comparison to previous literature

Our findings confirm and add to evidence from other PCD genotype-phenotype studies. The largest of these have been two cross-sectional and longitudinal studies from the USA and Canada (Genetic Disorders of Mucociliary Clearance Consortium) which also showed that patients with microtubular defects have worse lung function, based on ultrastructural phenotype and limited genotype information [8, 9]. We also confirmed associations previously described in smaller studies, such as the absence of situs inversus in individuals with radial spoke, central complex, N-DRC/molecular ruler gene mutations [4, 5, 22, 27, 28].

A previous study using lung clearance index as a more sensitive measure of lung function showed preserved lung function in a small group of patients from our cohort with normal ultrastructure, of which the majority have *DHAH11* defects [26]. We have further confirmed that this genotype is associated with milder lung disease by showing that these patients clustered in an area with higher values of FEV_1 z-scores. Traditional statistics also showed better preserved lung function in patients with *DNAH11* variants compared to those with mutations in any of the other genes.

Notably, patients carrying mutations in *DNAH5* were phenotypically diverse. The reasons for this are unclear, but may likely be connected to the variety of different mutations within this large gene. *DNAH5* was the gene found to have the widest spectrum of gene variants in our overall cohort. This diversity and high number of different mutations is in line with *DNAH5* being the commonest overall genetic cause of PCD and most frequently mutated gene in affected individuals, with at least 100 different pathogenic mutations recorded worldwide [29]. It is likely in PCD that there will be patient phenotypic differences associated not just with the specific gene, but also the nature and location of the mutations within that gene. These genotype related differences are already emerging on a smaller scale. For example in *DNAH5*, diagnostic results are known to vary somewhat depending on the mutation type, e.g. premature stop codon (nonsense) vs missense [30]. Differences are also associated with missense *versus* truncation mutations in *CCDC103*, where a milder diagnostic and clinical phenotype was described in individuals with p.His154Pro missense mutations [18].

Strengths and weaknesses

This is the largest study investigating genotype-phenotype associations in PCD to date. Using a new methodology of hypothesis-free TDA to examine underlying patterns in the dataset, genotype–phenotype patterns were identified from relatively few patients, something that would be difficult with usual clustering methods. The use of temporally and geographically distinct training and validation groups is highly recommended for such topological clustering approaches [31]. Initial UK discovery findings were validated in the mixed internal and external dataset, including by replication of several important previously published associations, suggesting these results are generalisable to other PCD populations.

The major weakness of our study remains the statistical power required to tease out relationships in a heterogeneous rare condition. To avoid problems with multiple comparisons and loss of statistical power, TDA-led hypothesis testing was performed for only two genes (*CCDC39* and *DNAH11*) and this required combining the discovery and validation datasets. A multinational dataset larger than any existing cohort will be required to ascertain further differences, especially to analyse whether variant types (stop-gain, frameshift, splicing, missense, copy number variants) explain some of the differences seen in the phenotypic data.

Another limitation of our study was potential recall bias for neonatal and early life events, with reliance on parental memory to report symptoms at the time of diagnosis. Not all medical records were complete and therefore missing data were recorded for some of these variables; however, TDA is particularly robust to missing data (see supplementary for additional information) [14]. Finally, we acknowledge that TDA is not completely hypothesis free, as we chose variables to enter into the models and there may be confounding variables affecting our models that have not been identified.

Potential impact for clinical management and research

A better understanding of genotype–phenotype associations from studies such as these should inform education and counselling for PCD patients and their families and will alter disease management in the future. Identifying patients that may require more aggressive or personalised treatment due to underlying genetics will allow for better and targeted care. High risk groups, such as patients with *CCDC39* mutations, might benefit from more intense and targeted therapies.

The identification of mutations in known PCD-causative genes confirms a diagnosis of PCD. The topological models highlighted previously described links between the affected gene, TEM defect and CBP from high-speed video analysis (HSVA), indicating that TEM and HSVA diagnostic tests can play an important supportive role in the classification (likely causal nature) of novel gene variants and variants of uncertain clinical significance [2,19]. These tests can also direct genetic testing to target a specific sub-set of genes.

Our approach for exploring genotype-phenotype associations might be useful for future longitudinal trials in PCD, by including longitudinal parameters such as lung function in the model. It is a model-generating approach that could also be usefully applied to other rare diseases and to more common conditions. More accurate mapping of clinical characteristics, including severity, will allow a more targeted approach to treatments, with associated improvements in patient outcomes.

Overall, these clinically important findings can be useful in counselling parents and when considering prognosis and ongoing therapeutic interventions.

Acknowledgements

We thank the patients and their families for participating in the study and acknowledge the PCD Family Support Group. Dr Borislav Dimitrov, University of Southampton, led initial discussions regarding statistical and TDA approaches to explore genotype-phenotype relationships. He sadly died before the analyses began. We thank the following for their clinical and laboratory contributions to data used in this manuscript: Lucy Jenkins, Thomas Cullup, Alexandros Onoufriadis, Patricia Goggin, Claire L Jackson, Janice Coles, James Thompson, Amanda Harris, Amanda Friend, Mellisa Dixon, Sarah Ollosson, Andrew V Rogers, Emily Frost, Charlotte Richardson, Farheen Daudvohra, Paul Griffin, Thomas Burgoyne. The researchers are supported by the BEAT-PCD: Better Evidence to Advance Therapeutic options for PCD network (COST Action 1407 and European Respiratory Society Clinical Research Collaboration). Several authors of this publication are members of the European Reference Network for Rare Respiratory Diseases (ERN-LUNG) - Project ID No 739546.

Figure legends

Figure 1. Study Design. TDA models were used to identify clusters of clinical and diagnostic characteristics. Gene groups and individual genes were mapped onto these clusters to develop hypotheses, which could subsequently be tested using traditional statistical approaches such as ANOVA. Without the use of TDA then comparison of FEV_1 across >20 genes would require multiple comparisons and statistical power would be lost, whereas using this method we were able to directly test a single directed-hypothesis.

Figure 2. Topological discovery model. Topology analysis display of the results of unbiased clustering of several levels of data, here showing the connections amongst the patients according to their underlying gene defect and the resulting cilia structure and motility defect. Each node represents combinations of features. The size of the nodes represents the number of subjects. The connections represent that there are patients shared between the two nodes. Models A-C are coloured by the following features: A. Gene group; B. Transmission electron microscopy (TEM) results; C. ciliary beat pattern (CBP) by high-speed video analysis (HSVA). Within each of the three models, patients are grouped according to five different classes of gene, TEM and CBP in each of the models respectively. CC= central complex defect, ODA = outer dynein arm, IDA = inner dynein arm, MTD = microtubular disorganisation. Asterisk indicates abbreviation for the nexin-dynein regulatory complex/molecular ruler group.

Figure 3. Topological discovery model. Each node represents combinations of features. The size of the nodes represents the number of subjects. The connections represent that there are patients shared between the two nodes. Models a-f are coloured by the following features: A. Gene group; B. FEV_1 z-scores; C. Neonatal respiratory distress syndrome (NRDS); D. *CCDC39*

mutations; E. *DNAH11* mutations; F. *DNAH5* mutations. Asterisk indicates abbreviation for the nexin-dynein regulatory complex/molecular ruler group.

Figure 4. Topological validation model. Each node represents combinations of features. The size of the nodes represents the number of subjects. The connections represent that there are patients shared between the two nodes. Models a-f are coloured by the following features: A. Gene group; B. FEV_1 z-scores; C. Neonatal respiratory distress syndrome (NRDS); D. *CCDC39* mutations; E. *DNAH11* mutations; F. *DNAH5* mutations. Asterisk indicates abbreviation for the nexin-dynein regulatory complex/molecular ruler group.

Figure 5. Total patient population according to genotype (n = 396). Mutations in 31 PCD genes were included for analysis. Bars are coloured according to gene group: blue represents genes involved in dynein structure, green in dynein assembly, yellow in radial spoke and central complex, orange in nexin-dynein regulatory complex/molecular ruler, and red in other functions such as ciliogenesis.

References

1. Goutaki, M., et al., *Clinical manifestations in primary ciliary dyskinesia: systematic review and meta-analysis.* Eur Respir J, 2016. **48**(4): p. 1081-1095.
2. Lucas, J.S., et al., *Primary ciliary dyskinesia in the genomics age.* Lancet Respir Med, 2020. **8**(2): p. 202-216.
3. Wallmeier, J., et al., *Motile ciliopathies.* Nat Rev Dis Primers, 2020. **6**(1): p. 77.
4. Olbrich, H., et al., *Recessive HYDIN mutations cause primary ciliary dyskinesia without randomization of left-right body asymmetry.* Am J Hum Genet, 2012. **91**(4): p. 672-84.
5. Castleman, V.H., et al., *Mutations in radial spoke head protein genes RSPH9 and RSPH4A cause primary ciliary dyskinesia with central-microtubular-pair abnormalities.* Am J Hum Genet, 2009. **84**(2): p. 197-209.
6. Boon, M., et al., *MCIDAS mutations result in a mucociliary clearance disorder with reduced generation of multiple motile cilia.* Nat Commun, 2014. **5**: p. 4418.
7. Best, S., et al., *Risk factors for situs defects and congenital heart disease in primary ciliary dyskinesia.* Thorax, 2019. **74**(2): p. 203-205.
8. Davis, S.D., et al., *Clinical features of childhood primary ciliary dyskinesia by genotype and ultrastructural phenotype.* Am J Respir Crit Care Med, 2015. **191**(3): p. 316-24.
9. Davis, S.D., et al., *Primary Ciliary Dyskinesia: Longitudinal Study of Lung Disease by Ultrastructure Defect and Genotype.* Am J Respir Crit Care Med, 2019. **199**(2): p. 190-198.
10. Lum, P.Y., et al., *Extracting insights from the shape of complex data using topology.* Scientific Reports, 2013. **3**.
11. Nielson, J.L., et al., *Topological data analysis for discovery in preclinical spinal cord injury and traumatic brain injury.* Nat Commun, 2015. **6**: p. 8581.
12. Frattini, V., et al., *A metabolic function of FGFR3-TACC3 gene fusions in cancer.* Nature, 2018. **553**(7687): p. 222-227.
13. Bruno, J.L., et al., *Longitudinal identification of clinically distinct neurophenotypes in young children with fragile X syndrome.* Proc Natl Acad Sci U S A, 2017. **114**(40): p. 10767-10772.
14. Offroy, M. and L. Duponchel, *Topological data analysis: A promising big data exploration tool in biology, analytical chemistry and physical chemistry.* Anal Chim Acta, 2016. **910**: p. 1-11.
15. Nicolau, M., A.J. Levine, and G. Carlsson, *Topology based data analysis identifies a subgroup of breast cancers with a unique mutational profile and excellent survival.* Proceedings of the National Academy of Sciences of the United States of America, 2011. **108**(17): p. 7265-7270.
16. Li, L., et al., *Identification of type 2 diabetes subgroups through topological analysis of patient similarity.* Sci Transl Med, 2015. **7**(311): p. 311ra174.
17. Siddiqui, S., et al., *Airway pathological heterogeneity in asthma: Visualization of disease microclusters using topological data analysis.* J Allergy Clin Immunol, 2018. **142**(5): p. 1457-1468.
18. Lucas, J.S., et al., *European Respiratory Society guidelines for the diagnosis of primary ciliary dyskinesia.* European Respiratory Journal, 2017. **49**(1): p. 1601090.
19. Richards, S., et al., *Standards and guidelines for the interpretation of sequence variants: a joint consensus recommendation of the American College of Medical Genetics and Genomics and the Association for Molecular Pathology.* Genet Med, 2015. **17**(5): p. 405-24.
20. Singh, G., F. Mémoli, and F. Carlsson, *Topological Methods for the Analysis of High Dimensional Data Sets and 3D Object Recognition*, in *Eurographics Symposium on Point Based Graphics*, M. Botsch, et al., Editors. 2007, The Eurographics Association. p. 91-100.
21. Glushakov, S. and I. Kotenko. *Handling Missing Data in Clinical Trials Using Topological Data Analysis*. 2018.

22. Pruliere-Escabasse, V., et al., *Otologic features in children with primary ciliary dyskinesia.* Arch Otolaryngol Head Neck Surg, 2010. **136**(11): p. 1121-6.
23. Wallmeier, J., et al., *Mutations in CCNO result in congenital mucociliary clearance disorder with reduced generation of multiple motile cilia.* Nat Genet, 2014. **46**(6): p. 646-51.
24. Davis, S.D., et al., *Clinical Features of Childhood Primary Ciliary Dyskinesia by Genotype and Ultrastructural Phenotype.* American Journal of Respiratory and Critical Care Medicine, 2015. **191**(3): p. 316-324.
25. Shah, A., et al., *A longitudinal study characterising a large adult primary ciliary dyskinesia population.* European Respiratory Journal, 2016. **48**(2): p. 441-450.
26. Irving, S., et al., *Primary Ciliary Dyskinesia Due to Microtubular Defects is Associated with Worse Lung Clearance Index.* Lung, 2018. **196**(2): p. 231-238.
27. Knowles, M.R., et al., *Mutations in RSPH1 cause primary ciliary dyskinesia with a unique clinical and ciliary phenotype.* Am J Respir Crit Care Med, 2014. **189**(6): p. 707-17.
28. Vallet, C., et al., *Primary ciliary dyskinesia presentation in 60 children according to ciliary ultrastructure.* Eur J Pediatr, 2013. **172**(8): p. 1053-60.
29. Landrum, M.J., et al., *ClinVar: improving access to variant interpretations and supporting evidence.* Nucleic Acids Res, 2018. **46**(D1): p. D1062-D1067.
30. Kispert, A., et al., *Genotype-phenotype correlations in PCD patients carrying DNAH5 mutations.* Thorax, 2003. **58**(6): p. 552-554.
31. Moons, K.G., et al., *Transparent Reporting of a multivariable prediction model for Individual Prognosis or Diagnosis (TRIPOD): explanation and elaboration.* Ann Intern Med, 2015. **162**(1): p. W1-73.

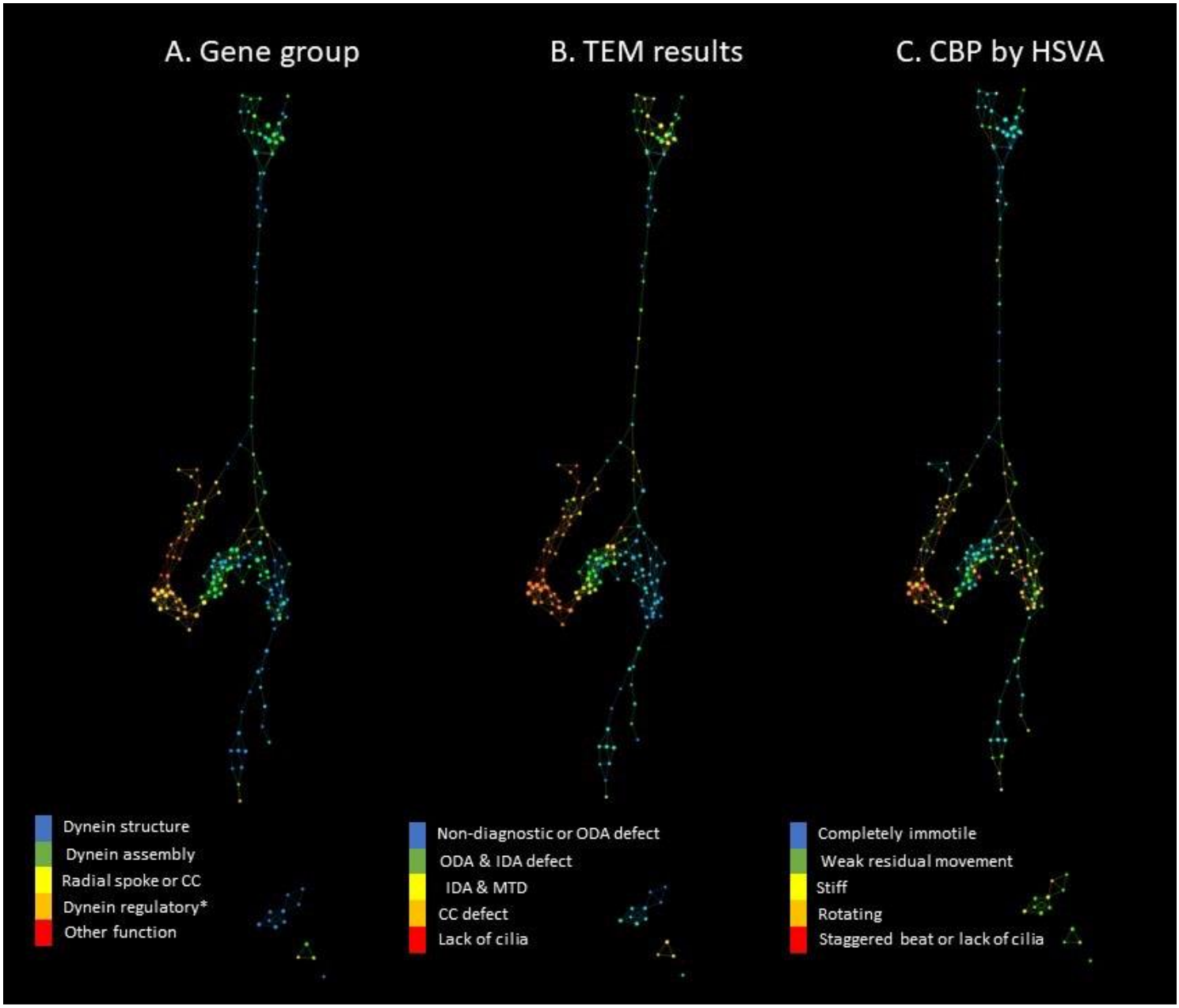
A. Gene group
B. TEM results
C. CBP by HSVA
Dynein structure
Dynein assembly
Radial spoke or CC
Dynein regulatory*
Other function
Non-diagnostic or ODA defect
ODA & IDA defect
IDA & MTD
CC defect
Lack of cilia
Completely immotile
Weak residual movement
Stiff
Rotating
Staggered beat or lack of cilia

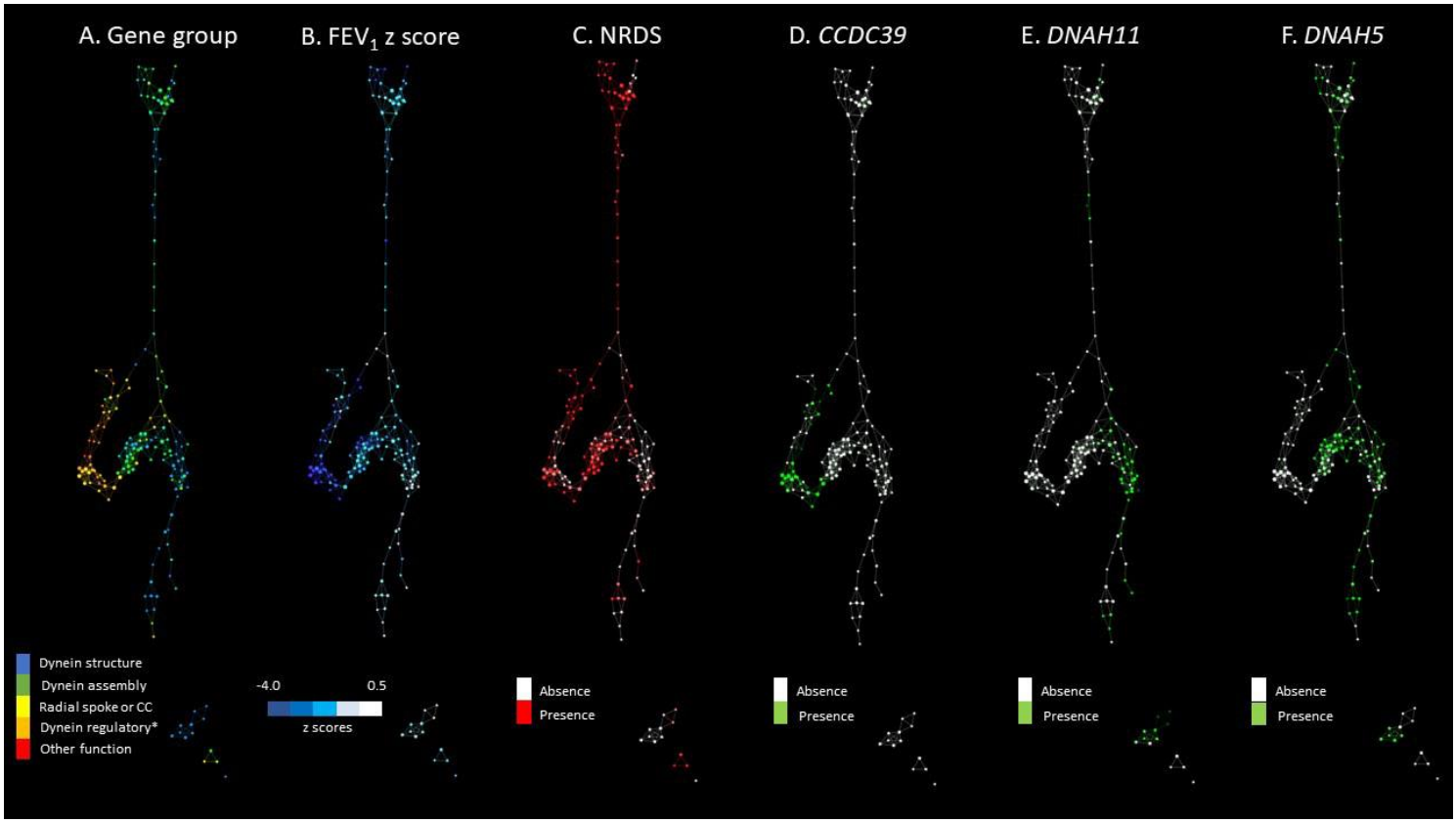
A. Gene group
B. FEV1 z score
C. NRDS
D. CCDC39
E. DNAH11
F. DNAH5
Dynein structure
Dynein assembly
Radial spoke or CC
Dynein regulatory*
Other function
-4.0
0.5
z scores
Absence
Presence
Absence
Presence
Absence
Presence
Absence
Presence

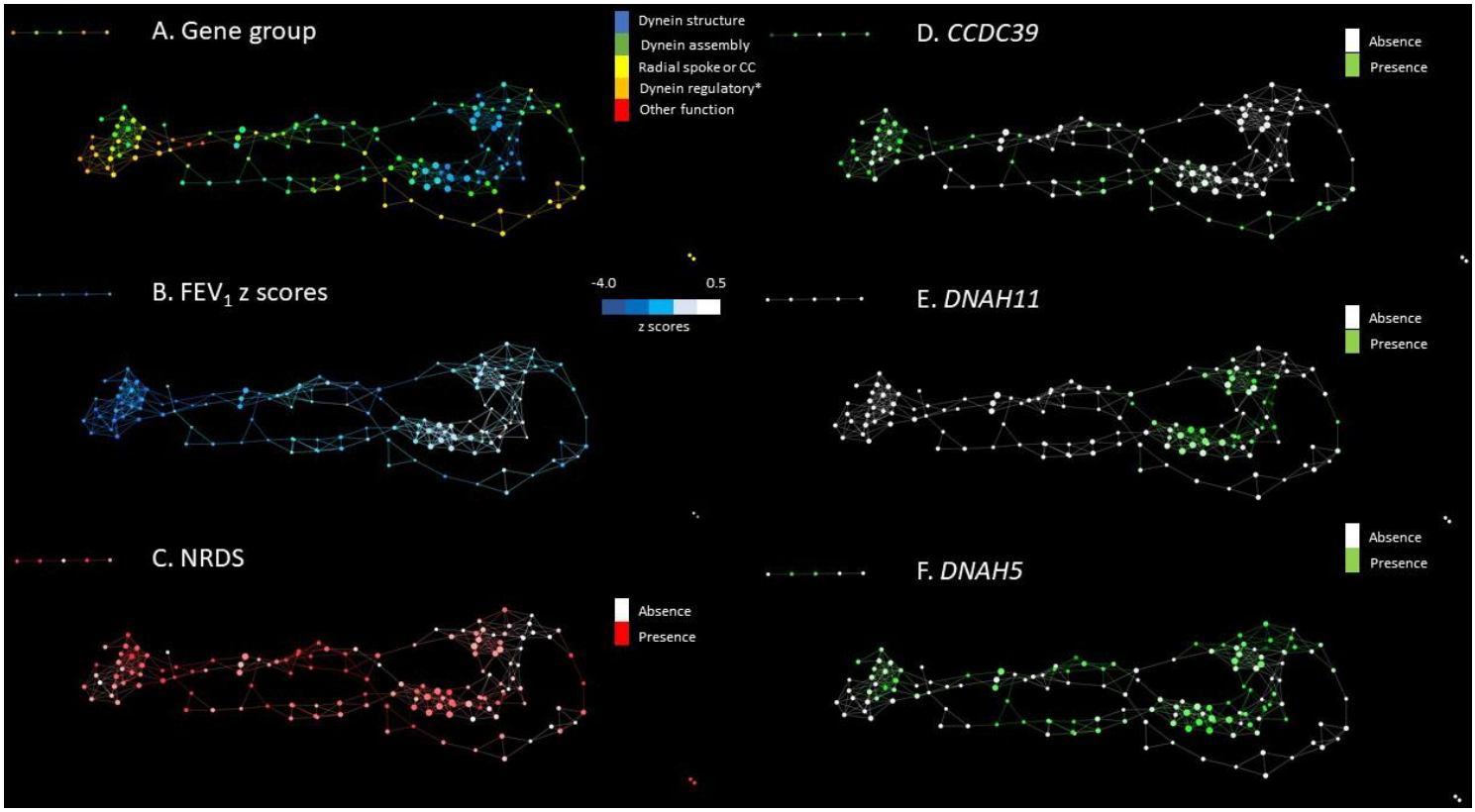
A. Gene group
Dynein structure
Dynein assembly
Radial spoke or CC
Dynein regulatory*
Other function
B. FEV1 z scores
-4.0
0.5
z scores
C. NRDS
Absence
Presence
D. CCDC39
Absence
Presence
E. DNAH11
Absence
Presence
F. DNAH5
Absence
Presence

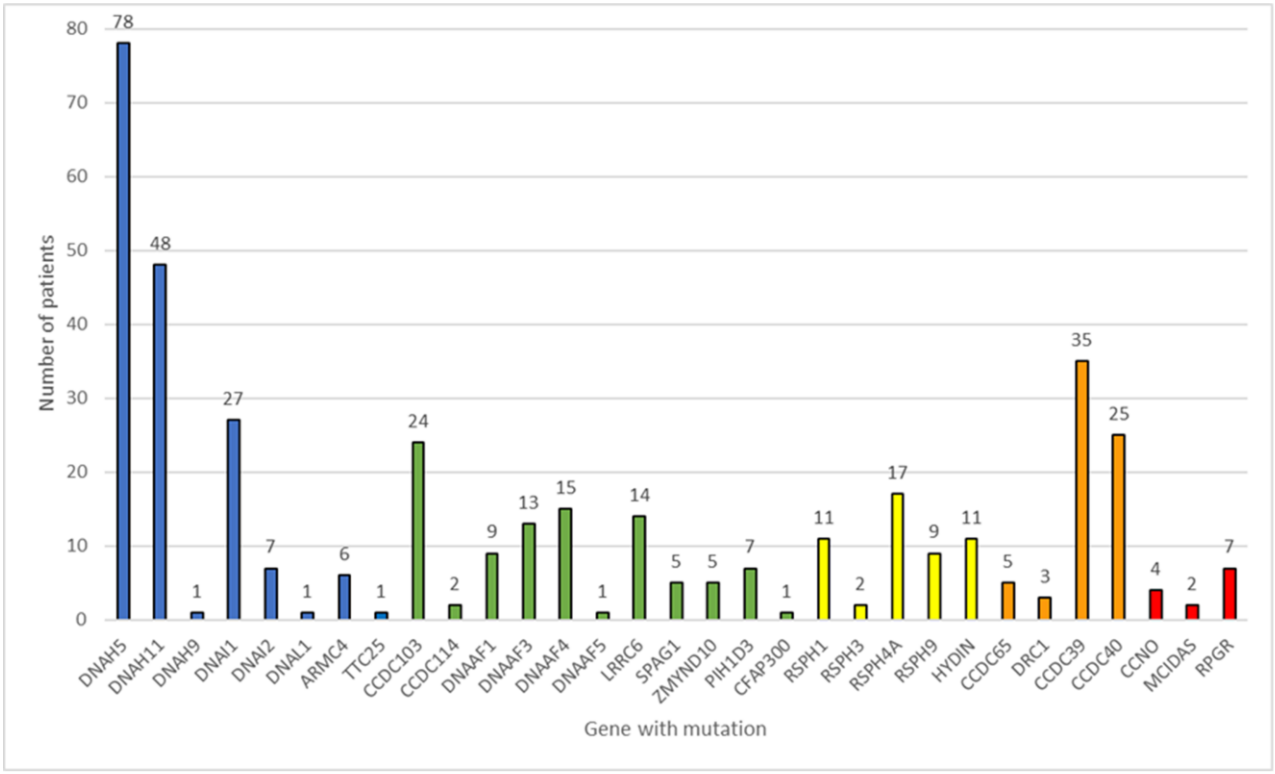
Number of patients
0
10
20
30
40
50
60
70
80
78
48
1
27
7
1
6
1
24
2
9
13
15
1
14
5
5
7
1
11
2
17
9
11
5
3
35
25
4
2
7
DNAH5
DNAH11
DNAH9
DNAI1
DNAI2
DNAL1
ARMC4
TTC25
CCDC103
CCDC114
DNAAF1
DNAAF3
DNAAF4
DNAAF5
LRRC6
SPAG1
ZMYND10
PIH1D3
CFAP300
RSPH1
RSPH3
RSPH4A
RSPH9
HYDIN
CCDC65
DRC1
CCDC39
CCDC40
CCNO
MCIDAS
RPGR
Gene with mutation

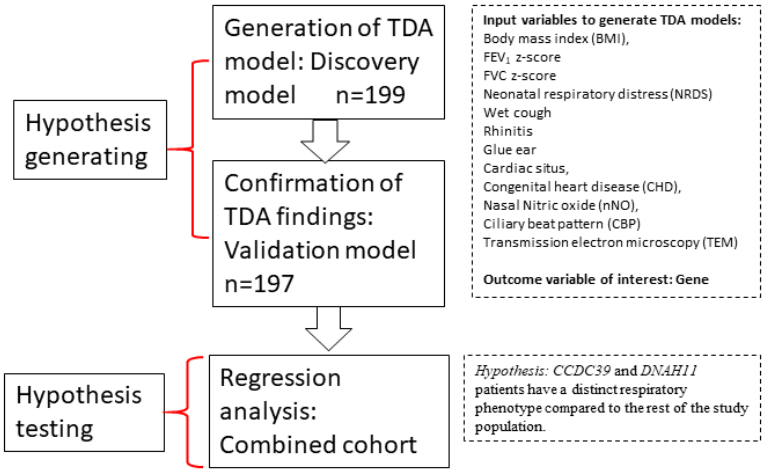
Hypothesis generating
Generation of TDA model: Discovery model n=199
Confirmation of TDA findings: Validation model n=197
Input variables to generate TDA models:
Body mass index (BMI),
FEV1 z-score
FVC z-score
Neonatal respiratory distress (NRDS)
Wet cough
Rhinitis
Glue ear
Cardiac situs,
Congenital heart disease (CHD),
Nasal Nitric oxide (nNO),
Ciliary beat pattern (CBP)
Transmission electron microscopy (TEM)
Outcome variable of interest: Gene
Hypothesis testing
Regression analysis: Combined cohort
Hypothesis: CCDC39 and DNAH11 patients have a distinct respiratory phenotype compared to the rest of the study population.

Supplementary methods

Ethics

Local and national research and ethical approvals were obtained and adhered to (NRES Committee South Central Hampshire Ethics 06/Q1702/109, London Bloomsbury Research Ethics Committee 08/H0713/82 and Ile-de-France Ethics Committee CPP07729).

Genetics

Patients were screened by the next generation and Sanger sequencing methods summarised. Genetic analysis was evaluated by geneticists and clinicians specialised in PCD, with a confirmed genetic diagnosis defined as the presence of autosomal bi-allelic or single X-linked hemizygous variants classified as pathogenic according to international guidelines [1, 2]. Of 292 genetically screened patients in the discovery cohort, using these criteria we confirmed a genetic diagnosis in 199 patients. We excluded 93 patients carrying variants judged to be of uncertain significance, which included single variants in PCD genes predicted pathogenic/likely pathogenic but without a second variant identified; variants identified in candidate rather than known PCD genes; and variants of uncertain pathogenic effect for example if TEM data inconsistent.

Discovery and validation cohorts

The discovery group consisted of PCD patients from University Hospital Southampton (UHS) and the Royal Brompton Hospital (RBH), London, genotyped at University College London (UCL). Clinical and diagnostic data were collected retrospectively from electronic and paper-

based medical records for all patients with a conclusive genetic result available up to July 2017. The validation group consisted of patients genotyped from UHS and RBH between July 2017 and May 2019, and at Trousseau, Cochin and Creteil hospitals in France and Emma Children's Hospital in the Netherlands up to May 2019. Study data were collected applying the definitions according to the study coding protocol. Ciliary beat pattern and TEM were reviewed by specialists, blinded to all genetic data.

The phenotypic data collected from both validation and discovery cohorts and used for clustering were based upon 12 clinical and diagnostic variables: BMI, FEV_1 z-score, FVC z-score, NRDS, wet cough, rhinitis, glue ear, cardiac situs, CHD, nNO, CBP and TEM, as described in the main manuscript. Data found not to shape the model during development were excluded; this include age at diagnosis, height, weight, mutation type and ethnicity. Additional data were collected on clinical and diagnostic characteristics (see Table E1) but were not included in the modelling; these were used to explore the model. Each variable was used to colour the nodes by the categories detailed in Table E1 to further explore potential clusters of phenotypic data.

Ciliary beat pattern was described and categorised according to the predominant finding from the following terms: normal, completely immotile, weak residual movement, stiff, rotating, staggered beat, lack of cilia. Transmission electron microscopy was categorised as one of the following terms: non diagnostic, isolated ODA defect, ODA & IDA defect, MTD & IDA defect or isolated IDA defect, CC defect or lack of cilia.

Topological data analysis (TDA)

Topology is a branch of applied mathematics that is primarily concerned with the study of shape of data and is specifically designed to identify structural characteristics of high-dimensional datasets. TDA [3] consists of a set of techniques for data analyses based on the reproduction of the structure of complex datasets into a geometric shape, that captures the essential features similarly to how a topographical map captures features of a landscape. It does so by dividing (or binning) the dataset through the application of a distance metric (e.g. a similarity measure) and then performing clustering within each of those separate segments. These are then visually represented as nodes of a network, each of which correspond to a collection of datapoints. TDA does not produce distinct clusters as traditional clustering techniques do but rather a network where points are connected depending on (dis)similarity between combination of the features of variables included in the model. In Symphony AyasdiAI, a user-friendly software that combines TDA with machine learning, different colours can be applied to the nodes of the network using any of the metrics or variables in the dataset, in order to inspect the data for patterns and hotspots.

TDA is an unsupervised data-driven technique, with no prior hypothesis needed. The outcome of interest should not be included in the clustering, which in this study were the genetic data. After the models were developed, we inspected the data by colouring the nodes by the different genes in order to identify any clusters or hotspots that would require further interrogation.

Machine learning was used in the lenses that were applied to our model. These lenses only provide the visualisation of the network through the application of a layout algorithm and therefore do not influence the clustering itself. In order to construct the topological models, we

applied a variety of lenses. Lenses can be derived from statistical measures such as mean, from geometry such as centrality, from dimensionality-reduction techniques such as principal component analysis (PCA), or even from a variable in the dataset. After exploring several different lenses, we selected locally linear embedding (LLE) lenses as the most relevant to our dataset because they showed distinct clusters for further exploration. Similarly, we selected correlation as a metric after evaluating other metrics. Correlation seemed an appropriate choice due to the differences of variance between variables, and the various categorical variables included in our dataset.

TDA deals with missing values individually; where they are missing, the TDA network will be mapped without that data point for that individual for that specific variable. The individual will still be plotted into the network according to similarities in variables for which there are data. For example, if an individual has values for BMI, NRDS, wet cough, rhinitis, glue ear, cardiac situs, CHD, nNO, CBP and TEM but data were missing for FEV_1 and FVC due to the age of the patient, this patient would be clustered in the TDA network according to similarities in the other ten variables for which we had measurements. This will have no effect on whether a patient clusters with patients that have similar values for these ten variables, they simply will not be clustered according to FEV_1 and FVC.

Additionally, TDA is highly robust in handling missing data, as has been shown in the literature [see references quoted in main paper] and also in a white paper by Glushakov et al [4]. In their study, the authors intentionally deleted values from their dataset in order to test the robustness of the TDA approach and found that the topological models were geometrically stable even when

90% of data were missing. We are therefore confident that missing data in our datasets did not affect the shape or clustering in the topological models.

Summary of clinical diagnostic methods by group

Method	University Hospital Southampton	Royal Brompton London	Hôpital Trousseau, Paris	Hôpital Intercommunal Créteil	Hôpital Kremlin-Bicêtre, Le Kremlin-Bicêtre	Hôpital Cochin, Paris	Amsterdam UMC
Genotyping	**Discovery group:** DNA extracted from blood using salting out technique and stored in -20 until further use. Next-generation sequencing performed as previously described [5], either by whole exome sequencing (WES) or targeted gene panel sequencing (Illumina TruSeq Custom Amplicon, Agilent SureSelect Focused Exome or SureSelectXT custom panel), including all known PCD genes and other candidate genes, on an Illumina platform. Variant analysis used an in-house bioinformatics pipeline similar to [6] with variant confirmation by Sanger sequencing with parental segregation. **Validation Group:** Wessex Clinical Exome analysis using the llumina TruSight One Sequencing Panel; 29 PCD gene panel applied to NGS sequence data. Confirmation by Sanger sequencing with parental segregation.	DNA extracted from blood using salting out technique and stored in -20 until further use. Next-generation sequencing performed as previously described [5], either by whole exome sequencing (WES) or targeted gene panel sequencing (Illumina TruSeq Custom Amplicon, Agilent SureSelect Focused Exome or SureSelectXT custom panel), including all known PCD genes and other candidate genes, on an Illumina platform. Variant analysis used an in-house bioinformatics pipeline similar to [6] with variant confirmation by Sanger sequencing with parental segregation. For a number of patients, variants were identified by candidate gene Sanger sequencing.	Genomic DNA was extracted from whole blood (EDTA sampling) either with the Maxwell 16 IVD device (Promega) or with a FlexiGene kit (Qiagen). DNA was analysed by a targeted capture panel (SeqCap EZ Choice, Roche Diagnostics) including all the known PCD genes and candidate genes. Librairies were sequenced on a MiSeq sequencer (Illumina). Data was analysed with a in-house double pipeline base on Bwa and Bowtie. Sequencing depth of the regions of interest was over 50X. DNA from relatives and control samples from the probands were analysed by Sanger sequencing (BigDye v3.1, Life Technologies) on a 3130XL sequencer (Life Technologies).	Performed in Hôpital Trousseau, Paris	Performed in Hôpital Trousseau, Paris	Performed in Hôpital Trousseau, Paris	DNA extracted from blood using a Chemogen robot and stored in -20 until further use. DNA sequencing was done using whole exome sequencing with targeted analysis, including all known PCD genes. Enriched libraries were sequenced with the HiSeq or Nextseq platforms (Illumina, San Diego, CA) as paired-end 100 bp reads. Sequencing reads were cleaned by 5′-end quality trimming and Illumina-adapter clipping by Trimmomatic. Prealignment quality control of the cleaned sequencing reads was done with FastQC. Clean reads were mapped to reference genome hg19 (GRCh37) using BWA-MEM. The genome analysis toolkit was used for recalibrating quality scores, realignment around indels, marking PCR duplicates, and variant calling and variants were annotated with

							ANNOVAR. All mutations were confirmed by Sanger sequencing. The analysis of the sequencing data was done using in-house bioinformatics pipeline. Sequencing and data analysis done at the Department of Clinical Genetics, Amsterdam UMC, Vrije Universiteit Amsterdam.
Nasal nitric oxide analysis	Ecomedics CLD 88 Exhalyzer; exhalation against resistance; sampling 0.33 l/min	Logan LR5000 Chemiluminscence Analyser (Rochester Kent); breath hold sampling 0.25 l/min	NIOX Flex up to 2014 ; From 2014 up to now CLD 88 sp Ecophysics chemiluminescence NO analyser ; sampling flow rate of 0.3 $L.min^{-1}$; measurements during breathhold, expiration against resistance and tidal breathing	EVA4000 chemiluminescent analyzer (Seres, France) ; breath hold sampling 1.3 l/min followed ATS/ERS standards	FeNO+ medisoft biochemical analyser (Sorinnes, Belgium), NO nasal at a sample flow rate of 100ml/s through a nasal catheter, breathing through resistance for velum closing	Chemiluminescence Analyser (EndoNO 8000®, SERES, Aix-en-Provence, France), breath hold analysis 1.3 l/min	Niox vero, exhalation against resistance, sampling 0.33l/min
Electron microscope	60,000x magnification (minimum) by Hitachi H7000; 100-300 cilia were imaged in transverse section for assessment of axonemal structure. Quantitative analysis determined ciliary ultrastructure.	60,000x magnification (minimum) by Hitachi H7000; 100-300 cilia were imaged in transverse section for assessment of axonemal structure. Quantitative analysis determined ciliary ultrastructure.	Performed in Hôpital Intercommunal Créteil	Analyses were carried out in the Pathology Department, in collaboration with the ICM-QUANT platform (Institut du Cerveau et de la Moelle Epinière, Paris). 80,000x magnification (minimum) by Hitachi HT7700; at least 100 cilia were imaged in transverse section for assessment of axonemal structure. Quantitative analysis determined ciliary ultrastructure.	Performed in Hôpital Intercommunal Créteil	Performed in Hôpital Intercommunal Créteil	The samples were screened by using a transmission electron microscope (Tecnai $12G^2$, FEI Company) and minimal 20 images of representative cross-sections were taken with a VELETA side-entry camera at a magnification of at least x60.000.
High-speed video microscopy equipment	0.5 mm coverwell imaging chamber (Sigma-Aldrich, Poole, UK) mounted onto a glass slide; Olympus IX71 inverted	0.5 mm coverwell imaging chamber (Sigma-Aldrich, Poole, UK) mounted onto a glass slide; Leica DM-LB upright microscope	Glass slide with coverslip; Nikon Eclipse Ci upright microscope with x100 oil plan objective lens; room temperature; PL-	Performed in Hôpital Trousseau, Paris	Performed in Hôpital Trousseau, Paris	Performed in Hôpital Trousseau, Paris	0.5 mm coverwell imaging chamber (Sigma-Aldrich, Poole, UK) mounted onto a glass slide; Zeiss AX10 Observer.A1 inverted

	microscope and condenser;x100 UPlan wide aperture oil objective; 37^{o}C heated environmental chamber (Solent Scientific, Southampton, UK); Photron FASTCAM MC2 high-speed video digital camera and Photron software.	with x100 oil plan objective lens; 37^{o}C heated stage; anti-vibration table (Wentworth Laboratories Ltd, Sandy, UK); Troubleshooter TS-5 Fastec imaging.	A741 high-speed video digital camera (PixeLINK, Ottawa, Canada).				microscope and condenser;Basler aVA1000 High-speed video digital camera and Strempix software.
High-speed video microscopy analyses	Images were digitally recorded using a high-speed camera at a rate of 500 frames per second (fps) and reviewed at reduced frame rates (30-60 fps) for analysis of ciliary beat pattern (CBP) and ciliary beat frequency (CBF).	Images were digitally recorded using a high-speed camera at a rate of 500 frames per second (fps) and reviewed at reduced frame rates (30-60 fps) for analysis of ciliary beat pattern (CBP) and ciliary beat frequency (CBF).	Images were digitally recorded using a high-speed camera at a rate of 355 frames per second (fps). Each movie was composed of 1,800 frames with a definition of 256 x 192 pixels (pixel size: 0.13 x 0.13 μm^2); twenty distinct areas containing intact undisrupted ciliated epithelial edges greater than 50 µm were recorded for analysis of ciliary beat pattern (CBP) and ciliary beat frequency (CBF).	Performed in Hôpital Trousseau, Paris	Performed in Hôpital Trousseau, Paris	Performed in Hôpital Trousseau, Paris	Images were digitally recorded using a high-speed camera at a rate of 120 frames per second (fps) and reviewed at reduced frame rates (10-20 fps) for analysis of ciliary beat pattern (CBP) and ciliary beat frequency (CBF).
Spirometry	FEV_1 on day of diagnostic testing, or first available result. Followed ATS/ERS Standards.	FEV_1 on day of diagnostic testing, or first available result. Followed ATS/ERS Standards.	FEV_1 on day of diagnostic testing, or first available result. Followed ATS/ERS Standards.	FEV_1 on day of diagnostic testing, or first available result. Followed ATS/ERS Standards.	FEV_1 on day of diagnostic testing, or first available result. Followed ATS/ERS Standards.	FEV_1 on day of diagnostic testing, or first available result. Followed ATS/ERS Standards. Jaeger MasterScreen Body (CAREFUSION, Hoechberg, Germany).	FEV_1 on day of diagnostic testing, or first available result. Followed ATS/ERS Standards.

Figure E1. Genetic results in 197 PCD patients from the *validation* group.

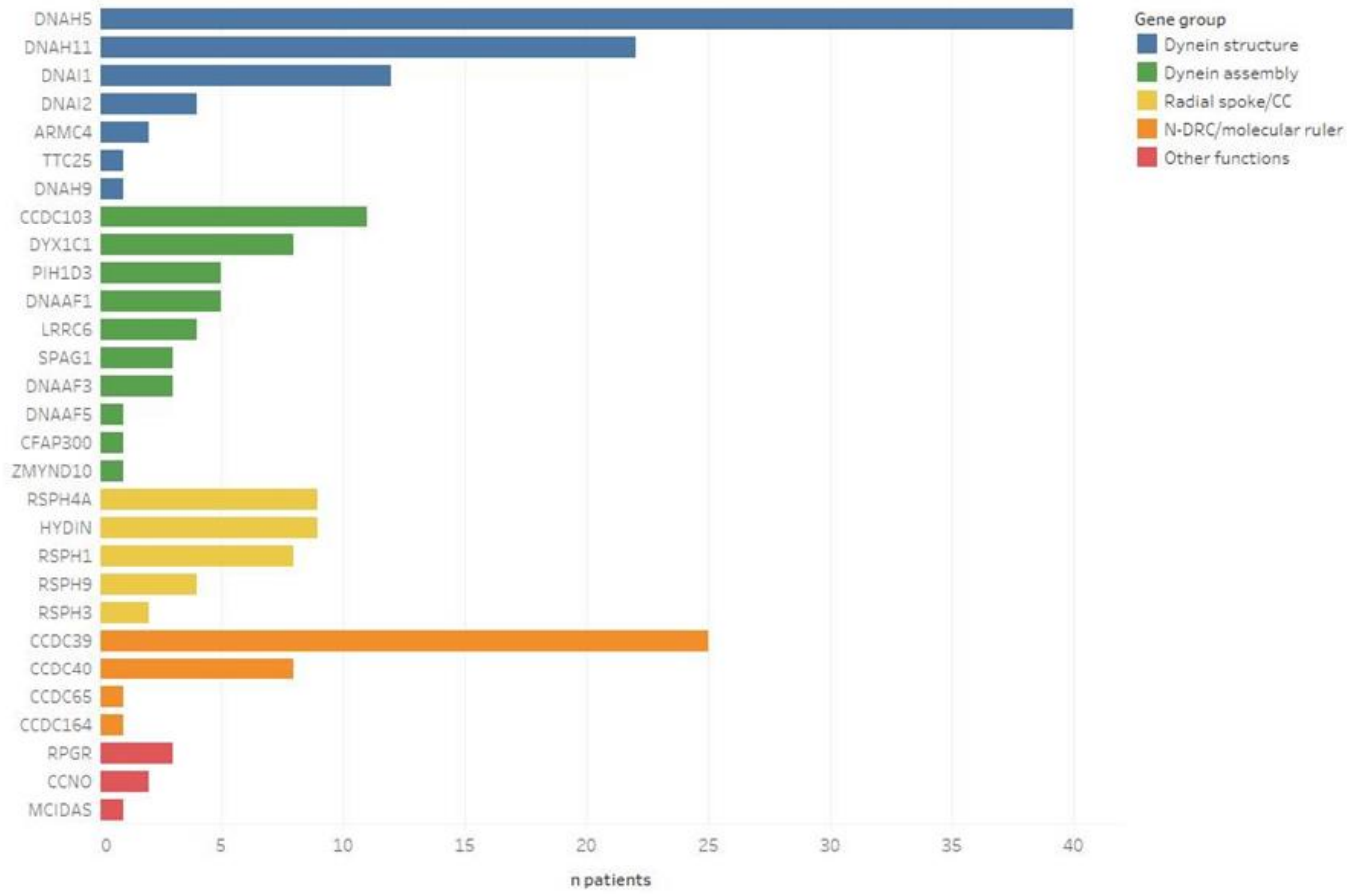

Patients in the validation cohort all had a confirmed clinical genetic diagnosis based upon PCD clinical experts identifying pathogenic or likely pathogenic variants, using identical diagnostic criteria for variant classification to that used for the discovery cohort (data not shown).

Figure E2. Stratification of all 31 PCD-causative genes in the overall study cohorts, placed into functional gene groups according to the ciliary components they encode.

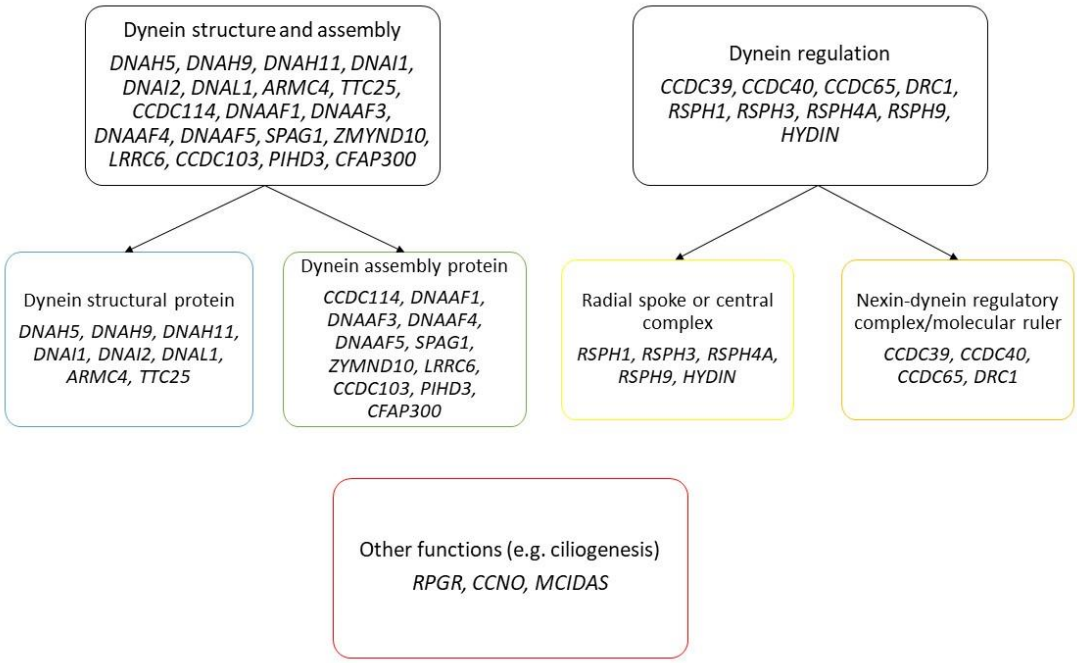

Each box defines a group: dynein structural protein, dynein assembly protein, radial spoke or central complex, dynein regulatory/molecular ruler, and other functions. Colours represent the gene groups: blue for genes involved in dynein structure, green in dynein assembly, yellow in radial spoke and central complex, orange in nexin-dynein regulatory complex/molecular ruler, and red in other functions.

Figure E3. Topological discovery model.

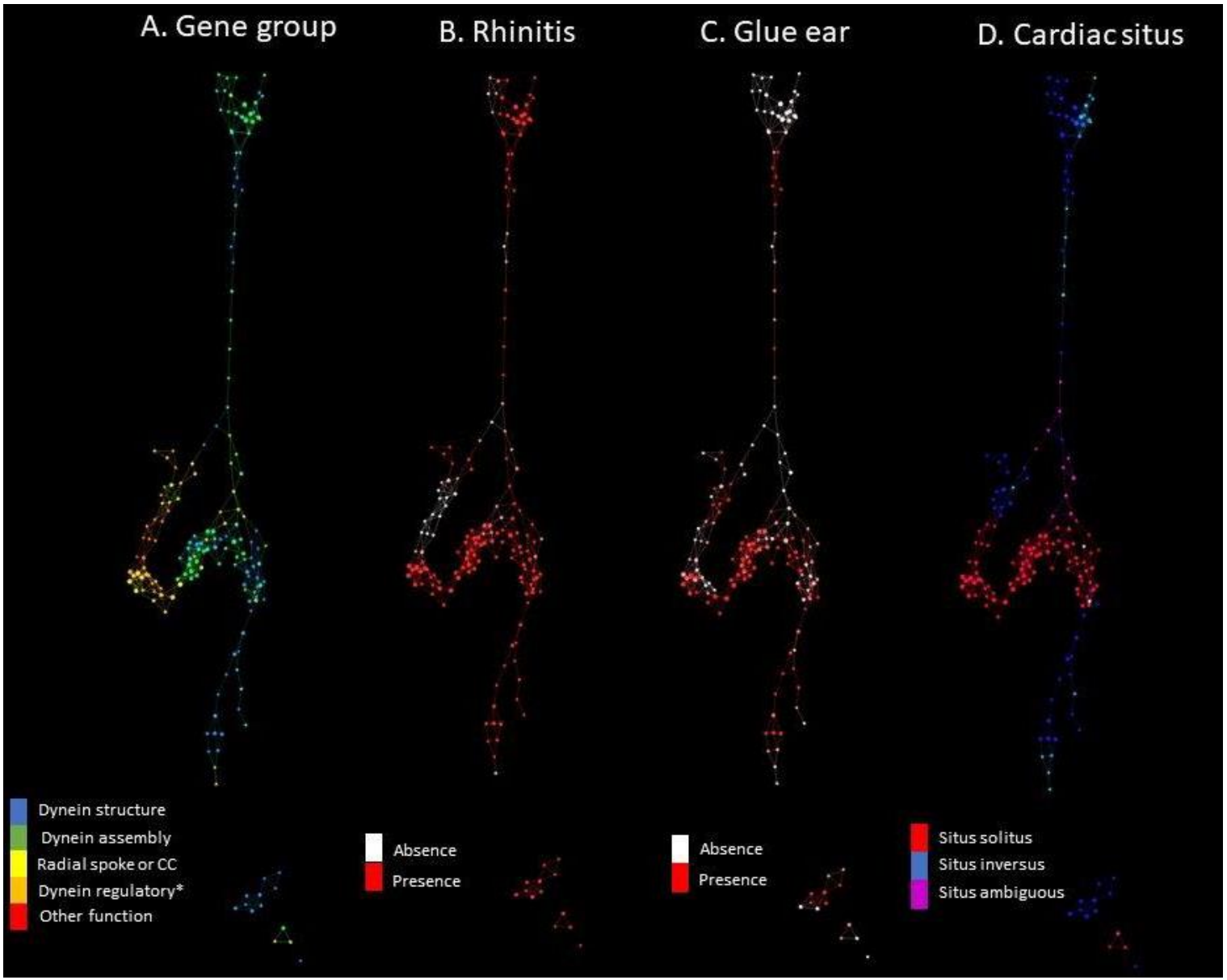

Models A-D are coloured by the following features: A. Gene group; B. History of rhinitis; C. History of glue ear; D. Cardiac situs. Node size represents the number of subjects. Each node represents combinations of features, connections represent that there are patients shared between the two nodes.

Figure E4. Topological validation model.

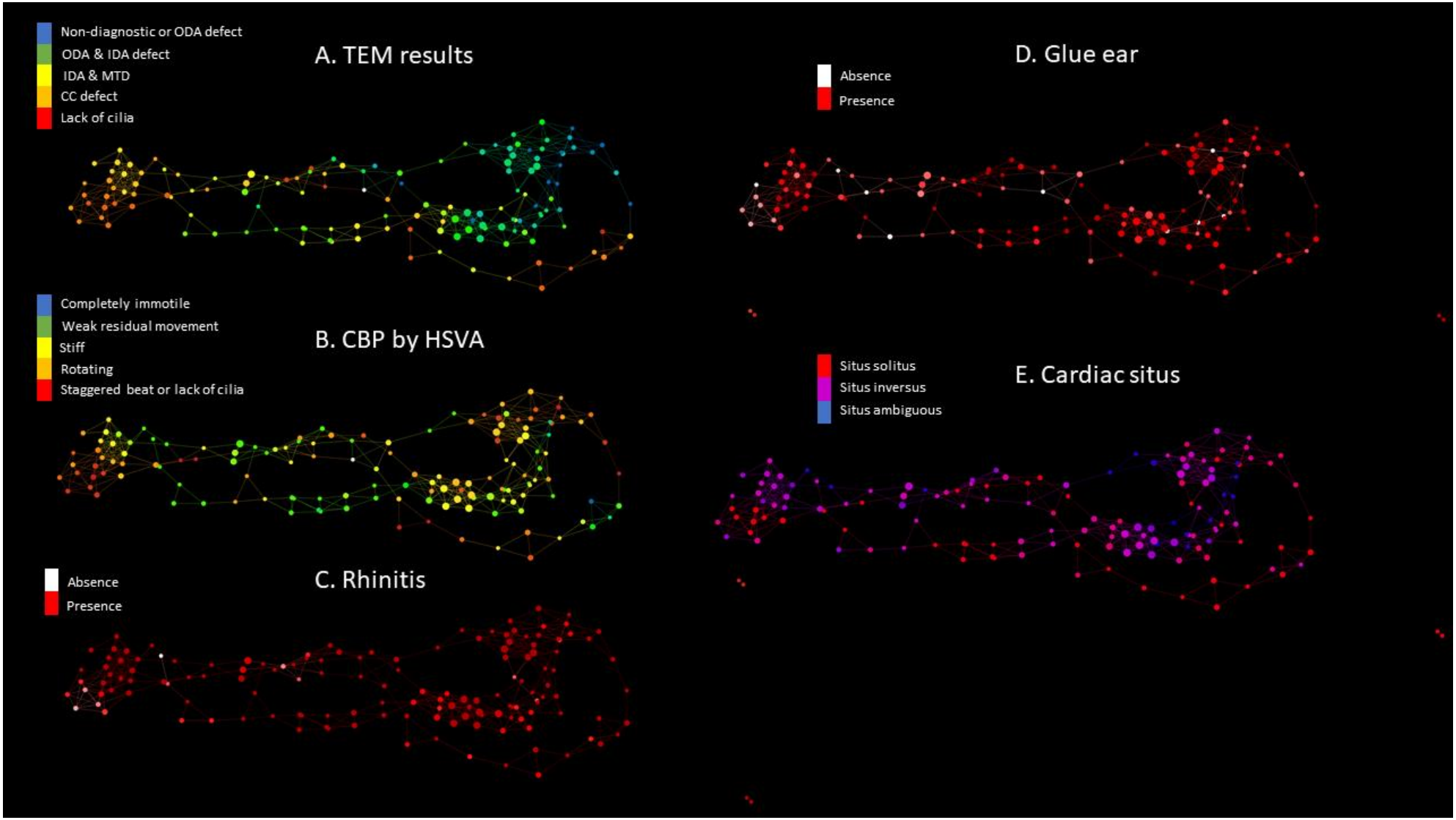

Models A-E are coloured by the following features: A. Transmission electron microscopy (TEM) findings; B. Ciliary beat pattern (CBP) by high-speed video analysis (HSVA); C. Rhinitis; D. Glue ear; E. Cardiac situs. Node size represents the number of subjects. Each node represents combinations of features, connections represent that there are patients shared between the two nodes.

Table E1. Description of data coding for clinical characteristics included in the study

Clinical characteristic	Description
Study ID	Unique ID (e.g. 0X-XXX)
DOB	
Date of LF (lung function) test	Closest to age at diagnosis Date format (e.g. DD-MM-YYYY)
Gender	Male = 1 Female = 2
Consanguinity	Up to 3rd degree cousins No = 0 Yes = 1
Number of siblings with PCD	Siblings with confirmed PCD
Ethnicity	Global Lung Function Initiative categories [7]
Weight	in kg
Height	in cm
BMI	Calculate BMI z-scores [8]
FEV_1	in litres. Calculate FEV_1 z-scores [7]
FVC	in litres
Date of diagnosis	Date format (e.g. DD-MM-YYYY)
Age at diagnosis	in years (1 decimal point)
Neonatal respiratory distress syndrome	Present Absent Unknown
History of wet cough	Present Absent Unknown
History of rhinitis	Present Absent

	Unknown
History of glue ear	Present Absent Unknown
Cardiac situs	Levocardia Dextrocardia Not applicable
Situs inversus totalis	Yes No Unknown
Echo done?	Yes No
Echo normal?	Yes No
Cardiac anatomy normal according to investigations?	Yes No Not applicable
Echo details, if abnormal	Free text
Abd USG	Performed Not performed
Abd USG normal?	Yes No Not applicable
nNO	in nL/min
Gene	Free text
Mutation	Free text
Transmission electron microscopy	
n cilia counted for arms	Calculate % of cilia with dynein arms
n cilia counted for microtubules	Calculate % of cilia with microtubules present
Both arms present	Calculate %

Inner arms missing	Calculate %
Outer arms missing	Calculate %
Both arms missing	Calculate %
Microtubular arrangement normal 9+2	Calculate %
Microtubules dis-arranged	Calculate %
Extra tubule	Calculate %
Single tubule	Calculate %
Central pair transposition	Calculate %
One of the central pair missing	Calculate %
Both central pair missing	Calculate %
Compound	Calculate %
TEM defect	Normal ODA IDA I&ODA IDA&MTD MTD Central complex defect Lack of cilia Inconclusive Note done
If ODA or I&ODA only please select if ODA is predominantly	Present Truncated Absent
If ODA or I&ODA only please select if ODA is present but not predominant	Present Truncated Absent
If ODA or I&ODA only please select if ODA is present but not predominant	Present Truncated Absent
High-speed video analysis	

CBP side view predominant finding	Normal Completely immotile Weak residual movement Stiff Rotating Staggered beat Long with bulbous tips Lack of cilia Not done
CBP present but not predominant 1	Normal Completely immotile Weak residual movement Stiff Rotating Staggered beat Long with bulbous tips Lack of cilia Not done
CBP present but not predominant 2	Normal Completely immotile Weak residual movement Stiff Rotating Staggered beat Long with bulbous tips Lack of cilia Not done
CBP present but not predominant 3	Normal Completely immotile Weak residual movement Stiff Rotating Staggered beat Long with bulbous tips Lack of cilia Not done
CBP present but not predominant 4	Normal Completely immotile Weak residual movement

	Stiff Rotating Staggered beat Long with bulbous tips Lack of cilia Not done
CBP present but not predominant 5	Normal Completely immotile Weak residual movement Stiff Rotating Staggered beat Long with bulbous tips Lack of cilia Not done
CBP present but not predominant 6	Normal Completely immotile Weak residual movement Stiff Rotating Staggered beat Long with bulbous tips Lack of cilia Not done
CBP top view predominant finding	Normal Completely immotile Weak residual movement Stiff Rotating Staggered beat Long with bulbous tips Lack of cilia Not done
CBP top present but not predominant 1	Normal Completely immotile Weak residual movement Stiff Rotating Staggered beat

	Long with bulbous tips Lack of cilia Not done
If stiff report location	Apical Basal Global
Syncronisation of CBP present	Yes No Not applicable
CBF	in Hz/min
Comments	Free text

Table E2. Diagnostic characteristics of patients in the *discovery* group, stratified by predefined gene groups. Genes are ordered according to gene distribution in the study population.

Diagnostic characteristic	**Dynein structure** (*DNAH5, DNAH11, DNAI1, ARMC4, DNAI2, DNAL1*) (n=89)	**Dynein assembly** (*CCDC103, DNAAF3, LRRC6, DNAAF4, SPAG1, ZYMND10, DNAAF1, CCDC114, PIHD3)* (n=52)	**Radial spoke or central complex** *(RSPH4A, RSPH9, RSPH1, HYDIN)* (n=18)	**N-RC/molecular ruler** *(CCDC40, CCDC39, DRC1, CCDC164)* (n=33)	**Other functions** *(RPGR, CCNO, MCIDAS)* (n=7)	**All**	**p-value**
Median nNO level in nL/min (IQR); n=149	11.0 (6.8 to 18.8)*	17.8 (7.8 to 33.6)	23.0 (11.0 to 34.2)	12.6 (5.4 to 18.8)	39.9 (15.3 to 96.9)*	13.0 (7.4 to 24.0)	**0.0071**
TEM findings, n=187							
Non-diagnostic TEM (%)	25 (30.1)	4 (7.7)	4 (23.5)	2 (6.9)	2 (33.3)	37 (19.8)	
Isolated ODA defect (%)	51 (61.5)	9 (17.3)	0	0	0	60 (32.1)	
ODA & IDA defect (%)	6 (7.2)	34 (65.4)	0	0	0	40 (21.4)	
MTD & IDA defect or isolated IDA defect (%)	0	4 (7.7)	0	27 (93.1)	0	31 (16.6)	
CC defect (%)	0	0	13 (76.5)	0	0	13 (7.0)	
Lack of cilia (%)	1 (1.2)	1 (1.9)	0	0	4 (66.7)	6 (3.2)	
CBP predominant side view, n=133							
Normal (%)	0	3 (8.8)	0	0	0	3 (2.7)	
Completely immotile (%)	35 (58.3)	25 (73.5)	0	5 (22.7)	3 (42.9)	68 (51.1)	
Weak residual movement (%)	8 (13.3)	0	0	1 (4.6)	0	9 (6.8)	

Stiff (%)	16 (26.7)	6 (17.7)	3 (30.0)	11 (50.0)	2 (28.6)	38 (28.6%	
Rotating (%)	0	0	7 (70.0)	0	0	7 (5.3)	
Staggered beat (%)	0	0	0	5 (22.7)	0	5 (3.8)	
Lack of cilia (%)	1 (1.7)	0	0	0	2 (28.6)	3 (2.3)	

*nNO= nasal nitric oxide (normal levels <77nl/min), TEM = Transmission electron microscopy, ODA= outer dynein arm, IDA = inner dynein arm, CC = central complex, CBP= ciliary beat pattern, ODA= outer dynein arm, IDA= inner dynein arm, MTD= microtubular disorganisation; * = significant difference between the pairs, Dunn's pairwise comparison with Holm-Sidak adjustment. P values ≤0.05 highlighted.

Table E3. Clinical characteristics of patients in the *discovery* group, stratified by predefined gene groups. Genes are ordered according to gene distribution in the study population.

Clinical characteristic	**Dynein structure** *(DNAH5, DNAH11, DNAI1, ARMC4, DNAI2, DNAL1)* (n=89)	**Dynein assembly** *(CCDC103, DNAAF3, LRRC6, DNAAF4, SPAG1, ZYMND10, DNAAF1, CCDC114 PIHD3)* (n=52)	**Radial spoke/ central complex** *(RSPH4A, RSPH9, RSPH1, HYDIN)* (n=18)	**N-DRC/molecular ruler** *(CCDC40, CCDC39, CCDC65, DRC1)* (n=33)	**Other functions** *(RPGR, CCNO, MCIDAS)* (n=7)	**All**	**p-value**
Male (%)	34 (38.2)	27 (51.9)	9 (50.0)	12 (36.4)	5 (71.4)	87 (43.7)	0.226
Ethnicity (n=191)							
White-British (%)	50 (58.1)	7 (13.5)	3 (16.7)	14 (50.0)	1 (14.3)	75 (39.3)	
White Irish (%)	0	5 (9.6)	3 (16.7)	1 (3.6)	4 (57.1)	13 (6.8)	
White-other (%)	10 (11.6)	4 (7.7)	1 (1.6)	5 (17.9)	1 (14.3)	21 (11.0)	
Indian (%)	4 (4.7)	5 (9.6)	0	1 (3.6)	0	10 (5.3)	
Pakistani (%)	6 (7.0)	18 (34.6)	3 (16.7)	2 (7.1)	0	29 (15.2)	
Bangladeshi (%)	0	2 (3.9)	1 (5.6)	0	0	3 (1.6)	
Sri Lankan (%)	3 (3.5)	2 (3.9)	0	0	0	5 (2.6)	
Middle East (%)	1 (1.2)	1 (1.9)	5 (27.8)	1 (3.6)	0	8 (4.2)	
Black (%)	7 (8.1)	0	1 (5.6)	1 (3.6)	0	9 (4.7)	
Chinese (%)	0	3 (5.8)	0	0	0	3 (1.6)	
Mixed (%)	1 (1.2)	1 (1.9)	0	1 (3.6)	0	3 (1.6)	
Other (%)	4 (4.7)	4 (7.9)	1 (5.6)	2 (7.1)	1 (14.3)	12 (6.3)	
Mean FEV_1 z-scores (SD), n=138	-1.4 (1.4) [+]	-1.9 (1.4)	-1.7 (2.1)	-2.7 (1.6) [+]	-2.7 (2.7)	-1.8 (1.6)	**0.0069**
Median age at diagnosis (IQR) n=184	9.1 (2.0 to 23.2)	7.3 (2.3 to 12.5)	9.5 (8.4 to 15.4)	7.5 2.0 to 13.8)	10.2 (5.8 to 12.7)	9.0 (2.9 to 15.4)	0.667
Neonatal respiratory distress (%)	31 (54.4)	31 (88.6)	7 (63.6)	15 (65.2)	3 (42.9)	87 (65.4)	**0.006**
Wet cough (%)	66 (94.3)	40 (100)	14 (100)	25 (96.2)	5 (71.4)	150 (95.5)	**0.042**
Rhinitis (%)	65 (91.6)	38 (95.0)	11 (91.7)	18 (72.0)	5 (71.4)	137 (88.4)	**0.027**

Glue ear (%)	38 (57.6)	19 (51.4)	9 (81.8)	9 (39.1)	4 (57.1)	79 (54.9)	0.206
Situs solitus (%)	31 (37.8)	19 (37.3)	18 (100)	18 (58.1)	7 (100%)	93 (49.2)	**<0.001**

[+] difference between groups was statistically significant (ANOVA followed by Tukey for pairwise comparisons). P values $\leq$0.05 highlighted.

Table E4. Variants defined in 199 PCD patients from the *discovery* cohort.

Pt ID	Gene	Allele 1	Allele 2	Variant classification		Reference	
				Allele 1	Allele 2	A1	A2
01-205	*ARMC4 (NM_001290020.1)*	c.1233_1234delinsT, p.Leu411Phefs*48	c.1969C>T, p.Gln657*	Frameshift (5)	Nonsense (5)	NA	[9]
01-214	*ARMC4 (NM_001290020.1)*	c.1283C>G, p.Ser428*	c.1283C>G, p.Ser428*	Nonsense (5)	Nonsense (5)	NA	NA
01-072	*ARMC4 (NM_001290020.1)*	c.2675C>A, p.Ser892*	c.2675C>A, p.Ser892*	Nonsense (5)	Nonsense (5)	[10]	[10]
01-073	*ARMC4 (NM_001290020.1)*	c.2675C>A, p.Ser892*	c.2675C>A, p.Ser892*	Nonsense (5)	Nonsense (5)	[10]	[10]
01-098	*CCDC103 (NM_001258395.1)*	c.461A>C, p.His154Pro	c.461A>C, p.His154Pro	Missense (5)	Missense (5)	[11-13]	[11-13]
01-099	*CCDC103 (NM_001258395.1)*	c.461A>C, p.His154Pro	c.461A>C, p.His154Pro	Missense (5)	Missense (5)	[11-13]	[11-13]
01-100	*CCDC103 (NM_001258395.1)*	c.461A>C, p.His154Pro	c.461A>C, p.His154Pro	Missense (5)	Missense (5)	[11-13]	[11-13]
01-103	*CCDC103 (NM_001258395.1)*	c.461A>C, p.His154Pro	c.461A>C, p.His154Pro	Missense (5)	Missense (5)	[11-13]	[11-13]
01-123	*CCDC103 (NM_001258395.1)*	c.461A>C, p.His154Pro	c.461A>C, p.His154Pro	Missense (5)	Missense (5)	[11-13]	[11-13]
01-124	*CCDC103 (NM_001258395.1)*	c.461A>C, p.His154Pro	c.461A>C, p.His154Pro	Missense (5)	Missense (5)	[11-13]	[11-13]
01-156	*CCDC103 (NM_001258395.1)*	c.461A>C, p.His154Pro	c.461A>C, p.His154Pro	Missense (5)	Missense (5)	[11-13]	[11-13]
01-170	*CCDC103 (NM_001258395.1)*	c.461A>C, p.His154Pro	c.461A>C, p.His154Pro	Missense (5)	Missense (5)	[11-13]	[11-13]
01-201	*CCDC103 (NM_001258395.1)*	c.461A>C, p.His154Pro	c.461A>C, p.His154Pro	Missense (5)	Missense (5)	[11-13]	[11-13]
02-051	*CCDC103 (NM_001258395.1)*	c.461A>C, p.His154Pro	c.461A>C, p.His154Pro	Missense (5)	Missense (5)	[11-13]	[11-13]
02-018	*CCDC103 (NM_001258395.1)*	c.461A>C, p.His154Pro	c.461A>C, p.His154Pro	Missense (5)	Missense (5)	[11-13]	[11-13]
02-033	*CCDC103 (NM_001258395.1)*	c.461A>C, p.His154Pro	c.461A>C, p.His154Pro	Missense (5)	Missense (5)	[11-13]	[11-13]
02-034	*CCDC103 (NM_001258395.1)*	c.461A>C, p.His154Pro	c.461A>C, p.His154Pro	Missense (5)	Missense (5)	[11-13]	[11-13]
01-079	*CCDC114 (NM_144577.3)*	c.287del, p.Lys96Argfs*23	c.287del, p.Lys96Argfs*23	Frameshift (5)	Frameshift (5)	NA	NA
01-029	*CCDC114 (NM_144577.3)*	c.486+1G>A	c.486+1G>A	Essential splice (5)	Essential splice (5)	[14]	[14]
01-074	*CCDC39 (NM_181426.1)*	c.1315A>T, p.Lys439*	c.1315A>T, p.Lys439*	Nonsense (5)	Nonsense (5)	NA	NA
01-064	*CCDC39 (NM_181426.1)*	c.1450del, p.Ile484Leufs*47	c.357+1G>C	Frameshift (5)	Essential splice (5)	[15]	[16]
01-030	*CCDC39 (NM_181426.1)*	c.1795C>T, p.Arg599*	c.1795C>T, p.Arg599*	Nonsense (5)	Nonsense (5)	[15]	[16]
01-045	*CCDC39 (NM_181426.1)*	c.2039_2040del, p.Cys680Phefs*9	c.526_527del, p.Leu176Alafs10*	Frameshift (5)	Frameshift (5)	[17]	NA
01-093	*CCDC39 (NM_181426.1)*	c.2040_2043del, p.Cys680Trpfs*15	c.440T>G, p.Leu147*	Frameshift (5)	Nonsense (5)	[17]	NA
01-063	*CCDC39 (NM_181426.1)*	c.2245G>T, p.Glu749*	c.2245G>T, p.Glu749*	Nonsense (5)	Nonsense (5)	[15]	[15]
01-016	*CCDC39 (NM_181426.1)*	c.2596G>T, p.Glu866*	c.2596G>T, p.Glu866*	Nonsense (5)	Nonsense (5)	[15]	[15]
02-028	*CCDC39 (NM_181426.1)*	c.664G>T, p.Glu222*	c.526_527del, p.Leu176Alafs10*	Nonsense (5)	Frameshift (5)	[15]	[15]
01-086	*CCDC39 (NM_181426.1)*	c.669_670insTA	c.610-2A>G	Frameshift (5)	Essential splice (5)	NA	[16]
01-200	*CCDC39 (NM_181426.1)*	c.830_831delCA, p.Asn276Lysfs*4	c.830_831delCA, p.Asn276Lysfs*4	Frameshift (5)	Frameshift (5)	[15]	[15]
01-102	*CCDC40 (NM_017950.3)*	c.1414del, p.Arg472Glyfs*3	c.3097A>T, p.Lys1033*	Frameshift (5)	Nonsense (5)	NA	[18]
01-179	*CCDC40 (NM_017950.3)*	c.1415delC, p.Arg472fs3*	c.1415delC, p.Arg472fs3*	Frameshift (5)	Frameshift (5)	[15]	[15]
02-049	*CCDC40 (NM_017950.3)*	c.1819_1823delinsT, p.Leu607Trpfs*33	c.1819_1823delinsT, p.Leu607Trpfs*33	Frameshift (5)	Frameshift (5)	NA	NA
01-138	*CCDC40 (NM_017950.3)*	c.248del, p.Ala83Valfs*84	c.552+6T>A	Frameshift (5)	Splice site (4)	[15, 19, 20]	[15, 19, 20]
01-054	*CCDC40 (NM_017950.3)*	c.248del, p.Ala83Valfs*84	c.248del, p.Ala83Valfs*84	Frameshift (5)	Frameshift (5)	[15, 19, 20]	[15, 19, 20]
01-068	*CCDC40 (NM_017950.3)*	c.248del, p.Ala83Valfs*84	c.248del, p.Ala83Valfs*84	Frameshift (5)	Frameshift (5)	[15, 19, 20]	[15, 19, 20]
02-045	*CCDC40 (NM_017950.3)*	c.248del, p.Ala83Valfs*84	c.248del, p.Ala83Valfs*84	Frameshift (5)	Frameshift (5)	[15, 19, 20]	[15, 19, 20]
02-067	*CCDC40 (NM_017950.3)*	c.248del, p.Ala83Valfs*84	c.748C>T, p.Glu250*	Frameshift (5)	Nonsense (5)	[15, 19, 20]	[15, 19, 20]
01-216	*CCDC40 (NM_017950.3)*	c.248del, p.Ala83Valfs*84	c.2450-2A>G	Frameshift (5)	Essential splice (5)	[15, 19, 20]	[15, 19, 20]
01-187	*CCDC40 (NM_017950.3)*	c.248del, p.Ala83Valfs*84	c.248del, p.Ala83Valfs*84	Frameshift (5)	Frameshift (5)	[15, 19, 20]	[15]
01-005	*CCDC40 (NM_017950.3)*	c.2712-1G>T	c.2712-1G>T	Essential splice (5)	Essential splice (5)	[15]	[15]
01-031	*CCDC40 (NM_017950.3)*	c.2712-1G>T	c.2712-1G>T	Essential splice (5)	Essential splice (5)	[15]	[15]
02-021	*CCDC40 (NM_017950.3)*	c.2712-1G>T	c.2712-1G>T	Essential splice (5)	Essential splice (5)	[15]	[15]
01-111	*CCDC40 (NM_017950.3)*	c.2712-1G>T	c.248del, p.Ala83Valfs*84	Essential splice (5)	Frameshift (5)	[15]	[15]
01-092	*CCDC40 (NM_017950.3)*	c.3181-3C>G	c.3181-3C>G	Splice site (3)	Splice site (3)	NA	NA
01-215	*CCDC40 (NM_017950.3)*	c.712G>T, p.Glu238*	c.940-2A>G	Nonsense (5)	Essential splice (5)	NA	[15]
01-137	*CCDC40 (NM_017950.3)*	c.940-2A>G	c.248del, p.Ala83Valfs*84	Essential splice (5)	Frameshift (5)	[15]	[15, 19, 20]

01-160	*CCDC65 (NM_033124.4)*	c.658G>T, p.Glu220*	c.658G>T, p.Glu220*	Nonsense (5)	Nonsense (5)	NA	NA
01-161	*CCDC65 (NM_033124.4)*	c.658G>T, p.Glu220*	c.658G>T, p.Glu220*	Nonsense (5)	Nonsense (5)	NA	NA
01-122	*CCDC65 (NM_033124.4)*	c.877_878del, p.Ile293Profs*2	c.877_878del, p.Ile293Profs*2	Frameshift (5)	Frameshift (5)	[21]	[21]
01-109	*CCDC65 (NM_033124.4)*	c.913C>T, p.Arg305*	c.913C>T, p.Arg305*	Nonsense (5)	Nonsense (5)	NA	NA
01-139	*CCNO (NM_021147.3)*	c.258_262dup, p.Gln88Argfs*8	c.258_262dup, p.Gln88Argfs*8	Frameshift (5)	Frameshift (5)	[22]	[22]
02-017	*CCNO (NM_021147.3)*	c.538dupC, p.Val180Glyfs*55	c.538dupC, p.Val180Glyfs*55	Frameshift (5)	Frameshift (5)	NA	NA
01-126	*DNAAF1 (NM_178452.5)*	c.285del, p.Lys95Asnfs*14	c.1484del, p.Pro495Glnfs*40	Frameshift (5)	Frameshift (5)	NA	[23]
01-127	*DNAAF1 (NM_178452.5)*	c.285del, p.Lys95Asnfs*14	c.1484del, p.Pro495Glnfs*40	Frameshift (5)	Frameshift (5)	NA	[23]
01-128	*DNAAF1 (NM_178452.5)*	c.285del, p.Lys95Asnfs*14	c.1484del, p.Pro495Glnfs*40	Frameshift (5)	Frameshift (5)	NA	[23]
01-223	*DNAAF1 (NM_178452.6)*	Deletion of exons 1-3	Deletion of exons 1-3	CNV (5)	CNV (5)	NA	NA
01-186	*DNAAF3 (NM_001256715.1)*	c.1030_1031delinsG, p.Pro344Glyfs*64	c.1273G>T, p.Gly425*	Frameshift (5)	Nonsense (5)	NA	NA
01-113	*DNAAF3 (NM_001256715.1)*	c.162_164delinsG, p.Val55Glyfs*28	c.162_164delinsG, p.Val55Glyfs*28	Frameshift (5)	Frameshift (5)	NA	NA
01-185	*DNAAF3 (NM_001256715.1)*	c.228+5G>C	c.228+5G>C	Splice site (3)	Splice site (3)	NA	NA
01-112	*DNAAF3 (NM_001256715.1)*	c.481-1G>A	c.481-1G>A	Essential splice (5)	Essential splice (5)	NA	NA
01-047	*DNAAF3 (NM_001256715.1)*	c.609_610delinsTGGGA, p.Ala272delinsGlyThr	c.296del, p.Glu167Glyfs*88	Inframe delins (5)	Frameshift (5)	NA	NA
01-089	*DNAAF3 (NM_001256715.1)*	c.621dupT, p.Val208Cysfs*12	c.621dupT, p.Val208Cysfs*12	Frameshift (5)	Frameshift (5)	[24]	[24]
01-090	*DNAAF3 (NM_001256715.1)*	c.621dupT, p.Val208Cysfs*12	c.621dupT, p.Val208Cysfs*12	Frameshift (5)	Frameshift (5)	[24]	[24]
01-174	*DNAAF3 (NM_001256715.1)*	c.621dupT, p.Val208Cysfs*12	c.621dupT, p.Val208Cysfs*12	Frameshift (5)	Frameshift (5)	[24]	[24]
01-131	*DNAAF3 (NM_001256715.1)*	c.901C>T, p.Gln301*	c.901C>T, p.Gln301*	Nonsense (5)	Nonsense (5)	NA	NA
01-070	*DNAAF3 (NM_001256715.1)*	c.997dup, p.Asp333Glyfs*64	c.570G>A, p.Trp190*	Frameshift (5)	Nonsense (5)	NA	NA
01-088	*DNAAF4 (NM_130810.3)*	3.5 kb deletion of exon 7	3.5 kb deletion of exon 7	CNV (5)	CNV (5)	[25]	[25]
01-232	*DNAAF4 (NM_130810.3)*	3.5 kb deletion of exon 7	3.5 kb deletion of exon 7	CNV (5)	CNV (5)	[25]	[25]
02-022	*DNAAF4 (NM_130810.3)*	3.5 kb deletion of exon 7	3.5 kb deletion of exon 7	CNV (5)	CNV (5)	[25]	[25]
02-010	*DNAAF4 (NM_130810.3)*	3.5 kb deletion of exon 7	3.5 kb deletion of exon 7	CNV (5)	CNV (5)	[25]	[25]
02-019	*DNAAF4 (NM_130810.3)*	3.5 kb deletion of exon 7	3.5 kb deletion of exon 7	CNV (5)	CNV (5)	[25]	[25]
01-085	*DNAAF4 (NM_130810.3)*	c.390_393del, p.Val132*	c.390_393del, p.Val132*	Nonsense (5)	Nonsense (5)	[25]	[25]
01-136	*DNAAF4 (NM_130810.3)*	c.808C>T, p.Arg270*	c.808C>T, p.Arg270*	Nonsense (5)	Nonsense (5)	[25]	[25]
01-176	*DNAH11 (NM_001277115.1)*	c.13040T>C, p.Leu4347Pro	Deletion of exons 68-75	Missense (3)	CNV (5)	NA	NA
02-073	*DNAH11 (NM_001277115.1)*	c.13270G>T, p.Glu4424*	c.13373C>T, p.Pro4458Leu	Nonsense (5)	Missense (5)	NA	[26]
01-040	*DNAH11 (NM_001277115.1)*	c.13531_13532ins13, p.Ala4511Valfs*13	c.3727G>T, p.Glu1243*	Frameshift (5)	Nonsense (5)	[27]	[27]
01-041	*DNAH11 (NM_001277115.1)*	c.13531_13532ins13, p.Ala4511Valfs*13	c.3727G>T, p.Glu1243*	Frameshift (5)	Nonsense (5)	[27]	[27]
01-042	*DNAH11 (NM_001277115.1)*	c.13531_13532ins13, p.Ala4511Valfs*13	c.3727G>T, p.Glu1243*	Frameshift (5)	Nonsense (5)	[27]	[27]
01-043	*DNAH11 (NM_001277115.1)*	c.13531_13532ins13, p.Ala4511Valfs*13	c.3727G>T, p.Glu1243*	Frameshift (5)	Nonsense (5)	[27]	[27]
01-095	*DNAH11 (NM_001277115.1)*	c.2832dup, p.Gln945Serfs*10	c.13240dup, p.Thr4414Asnfs*34	Frameshift (5)	Frameshift (5)	[27]	[27]
01-133	*DNAH11 (NM_001277115.1)*	c.3220G>T, p.Glu1074*	c.13069C>T, p.Arg4357*	Nonsense (5)	Nonsense (5)	[27]	[27]
01-147	*DNAH11 (NM_001277115.1)*	c.3380G>A, p.Trp1127*	c.3380G>A, p.Trp1127*	Nonsense (5)	Nonsense (5)	NA	NA
01-157	*DNAH11 (NM_001277115.1)*	c.3544C>T, p.Arg1182*	c.8798-5G>A	Nonsense (5)	Splice site (3)	[27]	[27]
02-063	*DNAH11 (NM_001277115.1)*	c.4333C>T, p.Arg1445*	c.9783G>C, p.Glu3261Asp	Nonsense (5)	Missense (3)	[26]	NA
02-062	*DNAH11 (NM_001277115.1)*	c.4333C>T, p.Arg1445*	c.4333C>T, p.Arg1445*	Nonsense (5)	Nonsense (5)	[26]	[26]
02-068	*DNAH11 (NM_001277115.1)*	c.4333C>T, p.Arg1445*	c.8698C>T, p.Arg2900*	Nonsense (5)	Nonsense (5)	[26]	[28]
02-038	*DNAH11 (NM_001277115.1)*	c.4333C>T, p.Arg1445*	c.13171C>T, p.Gln4391*	Nonsense (5)	Nonsense (5)	[26]	NA
01-065	*DNAH11 (NM_001277115.1)*	c.4410_4413del	c.7663C>T, p.Gln2555*	Frameshift (5)	Nonsense (5)	[27]	[27]
01-163	*DNAH11 (NM_001277115.1)*	c.4552C>T, p.Gln1518*	c.5778+1G>A, p.Val1821Thrfs*7	Nonsense (5)	Essential splice (5)	NA	[26]
01-084	*DNAH11 (NM_001277115.1)*	c.5506C>T, p.Arg1836*	c.5636T>A, p.Leu1879*	Nonsense (5)	Nonsense (5)	[27]	[27]
02-079	*DNAH11 (NM_001277115.1)*	c.5593C>T, p.Arg1865*	c.5593C>T, p.Arg1865*	Nonsense (5)	Nonsense (5)	NA	NA
01-158	*DNAH11 (NM_001277115.1)*	c.5924+1G>C	c.5924+1G>C	Essential splice (5)	Essential splice (5)	NA	NA
01-082	*DNAH11 (NM_001277115.1)*	c.6506C>T, p.Ser2169Leu	c.6506C>T, p.Ser2169Leu	Missense (3)	Missense (3)	[28]	[28]
01-083	*DNAH11 (NM_001277115.1)*	c.6506C>T, p.Ser2169Leu	c.6506C>T, p.Ser2169Leu	Missense (3)	Missense (3)	[28]	[28]
02-016	*DNAH11 (NM_001277115.1)*	c.6664C>T, p.Arg2222*	c.6682A>T, p.Lys2228*	Nonsense (5)	Nonsense (5)	NA	NA
01-221	*DNAH11 (NM_001277115.1)*	c.7472G>C, p.Arg2491Pro	c.6565C>T, p.Arg2189*	Missense (5)	Nonsense (5)	NA	NA
02-050	*DNAH11 (NM_001277115.1)*	c.8719C>T, p.Arg2907*	c.8719C>T, p.Arg2907*	Nonsense (5)	Nonsense (5)	[28]	[28]

01-169	*DNAH11 (NM_001277115.1)*	c.8932C>T, p.Gln2978*	c.853_857delinsG, p.Arg285Glufs*22	Nonsense (5)	Frameshift (5)	NA	NA
01-220	*DNAH11 (NM_001277115.1)*	c.9581_9582del, p.Leu3194Glnfs*10	c.4333C>T, p.Arg1445*	Frameshift (5)	Nonsense (5)	NA	[26]
01-178	*DNAH5 (NM_001369.2)*	c.10601T>C, p.Phe3534Ser	c.13458_13459insT, p.Asn4487fs*1	Missense (4)	Frameshift (5)	NA	[29, 30]
01-062	*DNAH5 (NM_001369.2)*	c.10616G>C, p.Arg3539Pro	c.7915C>T, p.Arg2639*	Missense (5)	Nonsense (5)	[31]	[32]
02-053	*DNAH5 (NM_001369.2)*	c.10815del, p.Pro3606Hisfs*22	c.6070-6071delAC, p.Gln2024Valfs*8	Frameshift (5)	Frameshift (5)	[20, 33, 34]	NA
02-054	*DNAH5 (NM_001369.2)*	c.10815del, p.Pro3606Hisfs*22	c.6070-6071delAC, p.Gln2024Valfs*8	Frameshift (5)	Frameshift (5)	[20, 33, 34]	NA
02-072	*DNAH5 (NM_001369.2)*	c.10815del, p.Pro3606Hisfs*22	c.5537T>C, p.Leu1846Pro	Frameshift (5)	Missense (5)	[20, 33, 34]	NA
02-048	*DNAH5 (NM_001369.2)*	c.10815del, p.Pro3606Hisfs*22	c.10616C>T, p.Arg3539Cys	Frameshift (5)	Missense (5)	[20, 33, 34]	[33]
02-023	*DNAH5 (NM_001369.2)*	c.10815del, p.Pro3606Hisfs*22	c.9720+5G>A	Frameshift (5)	Splice site (4)	[34]	NA
01-175	*DNAH5 (NM_001369.2)*	c.10815del, p.Pro3606Hisfs*22	c.13458_13459insT, p.Asn4487fs*1	Frameshift (5)	Frameshift (5)	[34]	[29, 30]
01-211	*DNAH5 (NM_001369.2)*	c.10815del, p.Pro3606Hisfs*22	c.10815del, p.Pro3606Hisfs*22	Frameshift (5)	Frameshift (5)	[33]	[33]
01-230	*DNAH5 (NM_001369.2)*	c.10815del, p.Pro3606Hisfs*22	c.2410G>T, p.Glu804*	Frameshift (5)	Nonsense (5)	[34]	NA
01-145	*DNAH5 (NM_001369.2)*	c.10825C>T, p.Gln3609*	c.3466del, p.Ile1156Leufs*24	Nonsense (5)	Frameshift (5)	NA	NA
01-146	*DNAH5 (NM_001369.2)*	c.10825C>T, p.Gln3609*	c.3466del, p.Ile1156Leufs*24	Nonsense (5)	Frameshift (5)	NA	NA
01-120	*DNAH5 (NM_001369.2)*	c.12705+1del	c.6249G>A, p.Met2083Ile	Essential splice (5)	Missense (5)	NA	[35]
01-191	*DNAH5 (NM_001369.2)*	c.13285C>T, p.Arg4429*	c.8642C>G, p.Ala2881Gly	Nonsense (5)	Missense (5)	NA	[34]
01-134	*DNAH5 (NM_001369.2)*	c.13285C>T, p.Arg4429*	c.13285C>T, p.Arg4429*	Nonsense (5)	Nonsense (5)	NA	NA
01-135	*DNAH5 (NM_001369.2)*	c.13285C>T, p.Arg4429*	c.13285C>T, p.Arg4429*	Nonsense (5)	Nonsense (5)	NA	NA
01-143	*DNAH5 (NM_001369.2)*	c.13338+1G>C	c.11437C>T, p.Arg3813Trp	Essential splice (5)	Missense (5)	NA	[18]
01-116	*DNAH5 (NM_001369.2)*	c.13399C>T, p.Gln4467*	c.13399C>T, p.Gln4467*	Nonsense (5)	Nonsense (5)	NA	NA
02-039	*DNAH5 (NM_001369.2)*	c.13458_13459insT, p.Asn4487fs*1	c.13338+1G>C	Frameshift (5)	Essential splice (5)	[29, 30]	NA
02-009	*DNAH5 (NM_001369.2)*	c.13458_13459insT, p.Asn4487fs*1	c.6930_6934delinsG, p.Asn2310Lysfs*15	Frameshift (5)	Frameshift (5)	[29, 30]	NA
01-048	*DNAH5 (NM_001369.2)*	c.13486C>T, p.Arg4496*	c.13458_13459insT, p.Asn4487fs*1	Nonsense (5)	Frameshift (5)	[29, 36, 37]	[29, 30]
02-024	*DNAH5 (NM_001369.2)*	c.13836G>A, p.Trp4612*	c.5710-2A>G, p.Cys1904-Lys1909del	Nonsense (5)	Essential splice (5)	NA	[33]
01-144	*DNAH5 (NM_001369.2)*	c.1828C>T, p.Gln610*	c.5563dup, p.Ile1855Asnfs*6	Nonsense (5)	Frameshift (5)	[32]	NA
01-189	*DNAH5 (NM_001369.2)*	c.232C>T, p.Arg78*	c.10815del, p.Pro3606Hisfs*22	Nonsense (5)	Frameshift (5)	[29, 36]	[34]
01-181	*DNAH5 (NM_001369.2)*	c.2710G>T, p.Glu904*	c.2710G>T, p.Glu904*	Nonsense (4)	Nonsense (4)	NA	NA
01-051	*DNAH5 (NM_001369.2)*	c.2893C>T, p.Gln965*	c.975-2A>G	Nonsense (5)	Essential splice (5)	NA	NA
01-206	*DNAH5 (NM_001369.2)*	c.5177T>C, p.Leu1726Pro	c.1730G>C, p.Arg577Thr	Missense (5)	Missense (5)	[31]	[29]
01-207	*DNAH5 (NM_001369.2)*	c.5177T>C, p.Leu1726Pro	c.1730G>C, p.Arg577Thr	Missense (5)	Missense (5)	[31]	[29]
02-029	*DNAH5 (NM_001369.2)*	c.5710-2A>G, p.Cys1904-Lys1909del	c.5710-2A>G, p.Cys1904-Lys1909del	Essential splice (5)	Essential splice (5)	[33]	[33]
01-190	*DNAH5 (NM_001369.2)*	c.5890_5894dup, p.Leu1966Serfs*9	c.6791G>A, p.Ser2264Asn	Frameshift (5)	Missense (5)	NA	[29]
02-011	*DNAH5 (NM_001369.2)*	c.6261T>G, p.Tyr2087*	c.6261T>G, p.Tyr2087*	Nonsense (5)	Nonsense (5)	NA	NA
02-026	*DNAH5 (NM_001369.2)*	c.6304C>T, p.Arg2102Cys	c.2052+1G>T	Missense (3)	Essential splice (5)	NA	NA
01-196	*DNAH5 (NM_001369.2)*	c.6763C>T, p.Arg2255*	c.9480T>A, p.Cys3160*	Nonsense (5)	Nonsense (5)	NA	NA
01-132	*DNAH5 (NM_001369.2)*	c.8383C>T, p.Arg2795*	c.5484+1G>A	Nonsense (5)	Essential splice (5)	NA	NA
01-209	*DNAH5 (NM_001369.2)*	c.8404C>T, p.Gln2802*	c.6249G>A, p.Met2083Ile	Nonsense (5)	Missense (5)	[29, 36]	NA
01-015	*DNAH5 (NM_001369.2)*	c.9516dup, p.Val3173Argfs*14	c.9516dup, p.Val3173Argfs*14	Frameshift (5)	Frameshift (5)	NA	NA
01-115	*DNAH5 (NM_001369.2)*	c.9694C>T, p.Gln3232*	c.9694C>T, p.Gln3232*	Nonsense (5)	Nonsense (5)	NA	NA
02-046	*DNAI1 (NM_012144.3)*	c.1490G>A, p.Gly497Asp	c.48+2dup, p.Ser17Valfs*12	Missense (5)	Essential splice (5)	[38]	[38]
01-044	*DNAI1 (NM_012144.3)*	c.1603del, p.Thr535Profs*31	c.1603del, p.Thr535Profs*31	Frameshift (5)	Frameshift (5)	NA	NA
01-069	*DNAI1 (NM_012144.3)*	c.1603del, p.Thr535Profs*31	c.1603del, p.Thr535Profs*31	Frameshift (5)	Frameshift (5)	NA	NA
01-087	*DNAI1 (NM_012144.3)*	c.1603del, p.Thr535Profs*31	c.1603del, p.Thr535Profs*31	Frameshift (5)	Frameshift (5)	NA	NA
02-013	*DNAI1 (NM_012144.3)*	c.1612G>A, p.Ala538Thr	c.1612G>A, p.Ala538Thr	Missense (5)	Missense (5)	[38]	[38]
02-031	*DNAI1 (NM_012144.3)*	c.1612G>A, p.Ala538Thr	c.1612G>A, p.Ala538Thr	Missense (5)	Missense (5)	[38]	[38]
01-021	*DNAI1 (NM_012144.3)*	c.48+2dup, p.Ser17Valfs*12	c.48+2dup, p.Ser17Valfs*12	Essential splice (5)	Essential splice (5)	[38]	[38]
01-022	*DNAI1 (NM_012144.3)*	c.48+2dup, p.Ser17Valfs*12	c.48+2dup, p.Ser17Valfs*12	Essential splice (5)	Essential splice (5)	[38]	[38]
01-140	*DNAI1 (NM_012144.3)*	c.48+2dup, p.Ser17Valfs*12	c.48+2dup, p.Ser17Valfs*12	Essential splice (5)	Essential splice (5)	[38]	[38]
02-006	*DNAI1 (NM_012144.3)*	c.48+2dup, p.Ser17Valfs*12	c.48+2dup, p.Ser17Valfs*12	Essential splice (5)	Essential splice (5)	[38]	[38]
02-058	*DNAI1 (NM_012144.3)*	c.48+2dup, p.Ser17Valfs*12	c.48+2dup, p.Ser17Valfs*12	Essential splice (5)	Essential splice (5)	[38]	[38]
02-059	*DNAI1 (NM_012144.3)*	c.48+2dup, p.Ser17Valfs*12	c.48+2dup, p.Ser17Valfs*12	Essential splice (5)	Essential splice (5)	[38]	[38]

02-069	*DNAI1 (NM_012144.3)*	c.48+2dup, p.Ser17Valfs*12	c.48+2dup, p.Ser17Valfs*12	Essential splice (5)	Essential splice (5)	[38]	[38]
01-001	*DNAI1 (NM_012144.3)*	c.48+2dup, p.Ser17Valfs*12	c.1612G>A, p.Ala538Thr	Essential splice (5)	Missense (5)	[38]	[38]
02-061	*DNAI1 (NM_012144.3)*	c.48+2dup, p.Ser17Valfs*12	c.1612G>A, p.Ala538Thr	Essential splice (5)	Missense (5)	[38]	[38]
01-028	*DNAI2 (NM_023036.4)*	c.1304G>A, p.Trp435*	c.1304G>A, p.Trp435*	Nonsense (5)	Nonsense (5)	[35]	[35]
01-101	*DNAI2 (NM_023036.4)*	c.1304G>A, p.Trp435*	c.1304G>A, p.Trp435*	Nonsense (5)	Nonsense (5)	[35]	[35]
01-229	*DNAI2 (NM_023036.4)*	c.883C>T, p.Arg295*	c.883C>T, p.Arg295*	Nonsense (5)	Nonsense (5)	NA	NA
01-097	*DNAL1 (NM_031427.3)*	c.225_229del, p.Leu75Phefs*30	c.225_229del, p.Leu75Phefs*30	Frameshift (5)	Frameshift (5)	NA	NA
01-055	*DRC1 (NM_145038.2)*	c.352C>T, p.Gln118*	c.2020C>T, p.Gln674*	Nonsense (5)	Nonsense (5)	[39]	NA
01-056	*DRC1 (NM_145038.2)*	c.352C>T, p.Gln118*	c.2020C>T, p.Gln674*	Nonsense (5)	Nonsense (5)	[39]	NA
01-119	*HYDIN (NM_001270974.2)*	c.13709del, p.Pro4570Leufs*22	c.13709del, p.Pro4570Leufs*22	Frameshift (5)	Frameshift (5)	NA	NA
01-121	*HYDIN (NM_001270974.2)*	c.2194dup, p.Tyr732Leufs*2	c.2194dup, p.Tyr732Leufs*2	Frameshift (5)	Frameshift (5)	NA	NA
02-027	*LRRC6 (NM_012472.4)*	c.299T>C, p.Ile100Thr	c.630del, p.Trp210Cysfs*12	Missense (5)	Frameshift (5)	[37]	[20]
01-057	*LRRC6 (NM_012472.4)*	c.630del, p.Trp210Cysfs*12	c.630del, p.Trp210Cysfs*12	Frameshift (5)	Frameshift (5)	[20]	[20]
01-094	*LRRC6 (NM_012472.4)*	c.630del, p.Trp210Cysfs*12	c.630del, p.Trp210Cysfs*12	Frameshift (5)	Frameshift (5)	[20]	[20]
01-129	*LRRC6 (NM_012472.4)*	c.630del, p.Trp210Cysfs*12	c.630del, p.Trp210Cysfs*12	Frameshift (5)	Frameshift (5)	[20]	[20]
01-130	*LRRC6 (NM_012472.4)*	c.630del, p.Trp210Cysfs*12	c.630del, p.Trp210Cysfs*12	Frameshift (5)	Frameshift (5)	[20]	[20]
01-184	*LRRC6 (NM_012472.4)*	c.630del, p.Trp210Cysfs*12	c.630del, p.Trp210Cysfs*12	Frameshift (5)	Frameshift (5)	[20]	[20]
01-204	*LRRC6 (NM_012472.4)*	c.630del, p.Trp210Cysfs*12	c.630del, p.Trp210Cysfs*12	Frameshift (5)	Frameshift (5)	[20]	[20]
01-218	*LRRC6 (NM_012472.4)*	c.630del, p.Trp210Cysfs*12	c.630del, p.Trp210Cysfs*12	Frameshift (5)	Frameshift (5)	[20]	[20]
01-010	*LRRC6 (NM_012472.4)*	c.183T>G, p.Asn61Lys	c.179-1G>A	Missense (4)	Essential splice (5)	NA	NA
01-011	*LRRC6 (NM_012472.4)*	c.183T>G, p.Asn61Lys	c.179-1G>A	Missense (4)	Essential splice (5)	NA	NA
01-142	*LRRC6 (NM_012472.4)*	c.793del, p.Arg266Aspfs*13	c.239_243del, p.Lys80Argfs*7	Frameshift (5)	Frameshift (5)	NA	NA
01-203	*MCIDAS (NM_001190787.1)*	c.332_333delinsG, p.Ala111Glyfs*22	c.332_333delinsG, p.Ala111Glyfs*22	Frameshift (5)	Frameshift (5)	NA	NA
01-007	*PIH1D3 (NM_001169154.1)*	c.127G>T, p.Glu43*	X-linked hemizygous	Nonsense (5)	-	[40]	-
01-164	*PIH1D3 (NM_001169154.1)*	c.266G>A, p.Trp89*	X-linked hemizygous	Nonsense (5)	-	[40]	-
01-075	*RPGR (NM_001034853.1)*	c.633del, p.Tyr212Metfs*11	X-linked hemizygous	Frameshift (5)	-	NA	-
02-007	*RPGR (NM_001034853.1)*	c.646G>T, p.Glu216*	X-linked hemizygous	Nonsense (5)	-	NA	-
02-012	*RPGR (NM_001034853.1)*	c.646G>T, p.Glu216*	X-linked hemizygous	Nonsense (5)	-	NA	-
02-037	*RPGR (NM_001034853.1)*	c.706C>T, p.Gln236*	X-linked hemizygous	Nonsense (5)	-	NA	-
01-208	*RSPH1 (NM_080860.3)*	c.275-2A>C, p.Gly92Alafs*10	c.275-2A>C, p.Gly92Alafs*10	Essential splice (5)	Essential splice (5)	[41]	[41]
02-005	*RSPH1 (NM_080860.3)*	c.275-2A>C, p.Gly92Alafs*10	c.275-2A>C, p.Gly92Alafs*10	Essential splice (5)	Essential splice (5)	[41]	[41]
02-008	*RSPH1 (NM_080860.3)*	c.275-2A>C, p.Gly92Alafs*10	c.275-2A>C, p.Gly92Alafs*10	Essential splice (5)	Essential splice (5)	[41]	[41]
01-199	*RSPH4A (NM_001010892.2)*	c.1351C>T, p.Gln451*	c.116C>A, p.Ser39*	Nonsense (5)	Nonsense (5)	NA	[42]
01-173	*RSPH4A (NM_001010892.2)*	c.1962_1966delinsC, p.Asp655Ilefs*83	c.1962_1966delinsC, p.Asp655Ilefs*83	Frameshift (5)	Frameshift (5)	NA	NA
01-026	*RSPH4A (NM_001010892.2)*	c.325C>T, p.Gln109*	c.1468C>T, p.Arg490*	Nonsense (5)	Nonsense (5)	[43]	[43]
01-037	*RSPH4A (NM_001010892.2)*	c.460C>T, p.Gln154*	c.460C>T, p.Gln154*	Nonsense (5)	Nonsense (5)	[43]	[43]
01-038	*RSPH4A (NM_001010892.2)*	c.460C>T, p.Gln154*	c.460C>T, p.Gln154*	Nonsense (5)	Nonsense (5)	[43]	[43]
01-039	*RSPH4A (NM_001010892.2)*	c.460C>T, p.Gln154*	c.460C>T, p.Gln154*	Nonsense (5)	Nonsense (5)	[43]	[43]
01-081	*RSPH4A (NM_001010892.2)*	c.460C>T, p.Gln154*	c.460C>T, p.Gln154*	Nonsense (5)	Nonsense (5)	[43]	[43]
02-057	*RSPH4A (NM_001010892.2)*	c.166dup, p.Arg56Profs*11	c.166dup, p.Arg56Profs*11	Frameshift (5)	Frameshift (5)	[12]	[12]
01-033	*RSPH9 (NM_001193341.1)*	c.801_803delGAA, p.Lys268del	c.801_803delGAA, p.Lys268del	Inframe AA del (5)	Inframe AA del (5)	[43]	[43]
01-034	*RSPH9 (NM_001193341.1)*	c.801_803delGAA, p.Lys268del	c.801_803delGAA, p.Lys268del	Inframe AA del (5)	Inframe AA del (5)	[43]	[43]
01-035	*RSPH9 (NM_001193341.1)*	c.801_803delGAA, p.Lys268del	c.801_803delGAA, p.Lys268del	Inframe AA del (5)	Inframe AA del (5)	[43]	[43]
01-036	*RSPH9 (NM_001193341.1)*	c.801_803delGAA, p.Lys268del	c.801_803delGAA, p.Lys268del	Inframe AA del (5)	Inframe AA del (5)	[43]	[43]
01-071	*RSPH9 (NM_001193341.1)*	c.801_803delGAA, p.Lys268del	c.801_803delGAA, p.Lys268del	Inframe AA del (5)	Inframe AA del (5)	[43]	[43]
01-194	*SPAG1 (NM_003114.4)*	c.1519dupA, p.Ile507Asnfs*5	c.1519dupA, p.Ile507Asnfs*5	Frameshift (5)	Frameshift (5)	[44]	[44]
01-195	*SPAG1 (NM_003114.4)*	c.1519dupA, p.Ile507Asnfs*5	c.1519dupA, p.Ile507Asnfs*5	Frameshift (5)	Frameshift (5)	[44]	[44]
01-025	*ZMYND10 (NM_015896.2)*	c.47T>G, p.Val16Gly	c.593_594del, p.Val198Glyfs*13	Missense (5)	Frameshift (5)	[45]	[45]
01-077	*ZMYND10 (NM_015896.2)*	c.65del, p.Phe22Serfs*21	c.65del, p.Phe22Serfs*21	Frameshift (5)	Frameshift (5)	[45]	[45]
01-078	*ZMYND10 (NM_015896.2)*	c.65del, p.Phe22Serfs*21	c.65del, p.Phe22Serfs*21	Frameshift (5)	Frameshift (5)	[45]	[45]
02-060	*ZMYND10 (NM_015896.2)*	c.47T>G, p.Val16Gly	c.47T>G, p.Val16Gly	Missense (5)	Missense (5)	[20, 45]	[20, 45]

Variants pathogenicity classified according to ACMG guidelines as Class 5 (pathogenic), Class 4 (likely pathogenic) or Class 3 (variant of uncertain significance, VUS) [2]. Class 3 variants (n=8) were included if variant present in combination with a Class 5 variant in the patient, or additional phenotypes suggested the Class 3 variant was highly likely causal although unpublished.

Table E5. Diagnostic characteristics of patients in the *validation* group, stratified by predefined gene groups. Genes are ordered according to gene distribution in the study population.

Diagnostic characteristic	**Dynein structure** *(DNAH5, DNAH11, DNAI1, DNAI2, ARMC4, DNAH9, TTC25)* (n=82)	**Dynein assembly** *(CCDC103, DNAAF4, PIHD3, DNAAF1, LRRC6, DNAAF3, SPAG1, DNAAF5, ZYMND10, CFAP300)* (n=42)	**Radial spoke/ central complex** *(RSPH4A, HYDIN, RSPH1, RSPH9, RSPH3)* (n=32)	**N-DRC/molecular ruler** *(CCDC39, CCDC40, CCDC65, DRC1)* (n=35)	**Other functions** *(RPGR, CCNO, MCIDAS)* (n=6)	**All**	**p-value**
Median nNO level in nL/min (IQR); n=138	16 (8.1 to 23.6)	14.4 (8 to 25)	22.9 (7.6 to 40.5)	13 (9.9 to 23)	35 (15.9 to 54)	16.3 (8.4 to 28)	0.7038
TEM findings, n=178							
Non-diagnostic TEM (%)	21 (28.4)	3 (8.3)	7 (22.6)	1 (2.9)	0	32 (18)	
Isolated ODA defect (%)	38 (51.4)	1 (2.8)	0	0	0	39 (21.9)	
ODA & IDA defect (%)	14 (18.9)	31 (86.1)	0	1 (2.9)	2 (66.7)	48 (27)	
MTD & IDA defect or isolated IDA defect (%)	0	1 (2.8)	1 (3.2)	32 (94.1)	0	34 (19.1)	
CC defect (%)	0	0	22 (71)	0	0	22 (12.4)	
Lack of cilia (%)	1 (1.4)	0	1 (3.2)	0	1 (33.3)	3 (1.7)	
CBP predominant side view, n=133							
Normal (%)	2 (2.6)	3 (9.1)	6 (20.7)	0	2 (40)	13 (7.4)	
Completely immotile (%)	34 (44.7)	27 (81.8)	1 (3.5)	14 (42.4)	1 (20)	77 (43.8)	
Weak residual movement (%)	29 (38.2)	3 (9.1)	6 (20.7)	12 (36.4)	0	50 (28.4)	
Stiff (%)	11 (14.5)	0	6 (20.7)	7 (21.2)	0	24 (13.6)	
Rotating (%)	0	0	10 (34.5)	0	0	10 (5.7)	
Staggered beat (%)	0	0	0	0	2 (40)	2 (1.1)	
Lack of cilia (%)	0	0	0	0	0	0	

*nNO= nasal nitric oxide (normal levels <77nl/min), TEM = Transmission electron microscopy, ODA= outer dynein arm, IDA = inner dynein arm, CC = central complex, CBP= ciliary beat pattern, ODA= outer dynein arm, IDA= inner dynein arm, MTD= microtubular disorganisation.

Table E6. Clinical characteristics of patients in the *validation* group, stratified by predefined gene groups. Genes are ordered according to gene distribution in the study population.

Clinical characteristic	**Dynein structure** *(DNAH5, DNAH11, DNAI1, DNAI2, ARMC4, DNAH9, TTC25)* (n=82)	**Dynein assembly** *(CCDC103, DNAAF4, PIHD3, DNAAF1, LRRC6, DNAAF3, SPAG1, DNAAF5, ZYMND10, CFAP300)* (n=42)	**Radial spoke/ central complex** *(RSPH4A, HYDIN, RSPH1, RSPH9, RSPH3)* (n=32)	**N-DRC/molecular ruler** *(CCDC39, CCDC40, CCDC65, DRC1)* (n=35)	**Other functions** *(RPGR, CCNO, MCIDAS)* (n=6)	**All**	**p-value**
Male (%)	41 (50)	22 (52.4)	14 (43.8)	23 (65.7)	4 (66.7)	104 (52.8)	0.393
Ethnicity, n=185							
White-British (%)	15 (20.0)	4 (11.1)	3 (9.4)	3 (9.4)	0	25 (13.5)	
White-Irish (%)	0	2 (5.6)	4 (12.5)	0	0	6 (3.2)	
White-other (%)	33 (41.8)	10 (27.8)	13 (40.6)	10 (31.3)	4 (66.7)	70 (37.8)	
Indian (%)	1 (1.3)	0	1 (3.1)	1 (3.1)	0	3 (1.6)	
Pakistani (%)	1 (1.3)	5 (13.9)	1 (3.1)	2 (6.3)	1 (16.7)	10 (5.4)	
Bangladeshi (%)	1 (1.3)	0	0	0	0	1 (0.5)	
Black (%)	2 (2.5)	3 (8.3)	1 (3.1)	1 (3.1)	0	7 (3.8)	
Chinese (%)	1 (1.3)	0	0	0	0	1 (0.5)	
Mixed (%)	5 (6.3)	0	0	1 (3.1)	0	6 (3.2)	
Other (%)	20 (25.3)	12 (33.3)	9 (28.1)	14 (43.8)	1 (16.7)	56 (30.3)	
Median FEV_1 z-scores (IQR), n=169	-1.3 (1.5)$^{+}$	-1.5 (1.6)	-2.1 (1.8)	-2.6 (1.5)$^{+}$	-2.6 (1.7)	-1.8 (1.6)	**0.0008**
Median age at diagnosis (IQR) n=184	14 (4.9 to 17.8)	14.3 (5.5 to 19.1)	15.9 (7.2 to 21.9)	13.9 (3.5 to 21.5)	20.4 (6.1 to 36)	14.5 (6 to 19.5)	0.435
Neonatal respiratory distress (%)	41 (56.9)	21 (60)	14 (50)	20 (69)	3 (50)	99 (58.2)	0.650
Wet cough (%)	78 (96.3)	38 (95)	29 (93.6)	31 (91.2)	5 (83.3)	181 (94.3)	0.431
Rhinitis (%)	77 (96.3)	37 (90.2)	26 (83.9)	31 (91.2)	5 (83.3)	176 (91.7)	0.150
Glue ear (%)	55 (69.6)	26 (66.7)	25 (83.3)	23 (69.7)	4 (66.7)	133 (71.1)	0.574
Situs solitus (%)	38 (48.1)	17 (41.5)	30 (100)	22 (62.9)	6 (100)	113 (59.2)	**<0.001**

$^{+}$ difference between groups was statistically significant (ANOVA followed by Tukey for pairwise comparisons). P values ≤0.05 highlighted. IQR: interquartile range, NRDS: neonatal respiratory distress syndrome, CHD: congenital heart defect.

Table E7. Summary of diagnostic test results for all patients included in the study, stratified by gene group. Genes are ordered according to gene distribution in the study population.

Diagnostic test	**Dynein structure** *(DNAH5, DNAH11, DNAI1, DNAI2, ARMC4, DNAL1, DNAH9, TTC25)*, (n=171)	**Dynein assembly** *(CCDC103, DNAAF4, LRRC6, DNAAF3, DNAAF1, PIHD3, SPAG1, ZYMND10, CCDC114, DNAAF5, CFAP300)*, (n=94)	**Radial spoke/ central complex** *(RSPH4A, RSPH1, HYDIN, RSPH9, RSPH3)*, (n=50)	**N-DRC/molecular ruler** *(CCDC39, CCDC40, CCDC65, DRC1)*, (n=68)	**Other function** *(RPGR, CCNO, MCIDAS)*, (n=13)	**All**
nNO findings (%), n=287						
Median nNO level in nL/min [IQR]; n=287	12.1 [7.2 to 21.3]	15.3 [7.9 to 30.4]	23 [9.8 to 36]	12.8 [7.5 to 20]	39.9 [15.6 to 75.5]	14.4 [8.0 to 26.0]
n patients with nNO<77 nL/min (%)	120 (95.2)	53 (88.3)	34 (89.5)	54 (98.2)	6 (75)	267 (93.0)
TEM findings (%), n=365						
Non-diagnostic TEM	46 (29.3)	7 (8.0)	10 (20.8)	3 (4.8)	2 (22.2)	68 (18.6)
Isolated ODA defect	89 (56.7)	10 (11.4)	0	0	0	99 (27.1)
ODA & IDA defect	20 (12.7)	65 (73.9)	0	1 (1.6)	(22.2)	88 (24.1)
MTD & IDA defect or isolated IDA defect	0	5 (5.7)	1 (2.1)	59 (93.7)	0	65 (17.8)
CC defect	0	0	35 (72.9)	0	0	35 (9.6)
Lack of cilia	2 (1.3)	1 (1.1)	2 (4.2)	0	5 (55.6)	10 (2.7)
CBP predominant side view (%), n=309						
Normal	2 (1.5)	6 (9.0)	6 (15.4)	0	2 (16.7)	16 (5.2)
Completely immotile	69 (50.7)	52 (77.6)	1 (2.6)	19 (34.6)	4 (33.3)	145 (46.9)
Weak residual movement	37 (27.2)	3 (4.5)	6 (15.4)	13 (23.6)	0	59 (19.1)
Stiff	27 (19.9)	6 (9.0)	9 (23.1)	18 (32.7)	2 (16.7)	62 (20.1)
Rotating	0	0	16 (41.0)	0	0	16 (5.2)
Staggered beat	0	0	1 (2.6)	5 (9.1)	2 (16.7)	8 (2.6)
Lack of cilia	1 (0.7)	0	0	0	2 (16.7)	3 (1.0)

N-DRC = nexin-dynein regulatory complex, nNO = nasal nitric oxide (normal levels <77nl/min), IQR = interquartile range, TEM = Transmission electron microscopy, ODA= outer dynein arm, IDA = inner dynein arm, CC = central complex, MTD = microtubular disorganisation, CBP= ciliary beat pattern.

Table E8. Summary of clinical characteristics for all patients included in the study, stratified by gene group. Genes are ordered according to gene distribution in the study population.

Clinical characteristic	**Dynein structure** *(DNAH5, DNAH11, DNAI1, DNAI2, ARMC4, DNAL1, DNAH9, TTC25)*, (n=171)	**Dynein assembly** *(CCDC103, DNAAF4, LRRC6, DNAAF3, DNAAF1, PIHD3, SPAG1, ZYMND10, CCDC114, DNAAF5, CFAP300)*, (n=94)	**Radial spoke/ central complex** *(RSPH4A, RSPH1, HYDIN, RSPH9, RSPH3)*, (n=50)	**N-DRC/ molecular ruler** *(CCDC39, CCDC40, CCDC65, DRC1)*, (n=68)	**Other function** *(RPGR, CCNO, MCIDAS)*, (n=13)	**All**	**p-value**
Male (%), n=396	75 (43.9)	49 (52.1)	23 (46.0)	35 (51.5)	9 (69.2)	191 (48.2)	0.226
Mean FEV_1 z-scores (SD), n=275	-1.3 (1.4)$^{+}$	-1.7 (1.5)$^{\#}$	-1.7 (1.9)	-2.5 (1.5)$^{+\#}$	-2.8 (2.2)	-1.7 (1.6)	**<0.001**
Median age at diagnosis (IQR) n=353	12 (3 to 20)	9.6 (3.1 to 16.3)	14.6 (7.8 to 18.7)	10.9 (2.2 to 15.4)	12.1 (6 to 20.4)	11.1 (4.2 to 17.8)	0.235
Neonatal respiratory distress syndrome (%), n=305	72 (55.8)	52 (73.2)	21 (52.5)	35 (67.3)	6 (46.2)	186 (61.0)	0.056
Wet cough (%), n=351	144 (95.4)	78 (95.3)	43 (93.5)	56 (93.3)	10 (76.9)	331 (94.3)	0.165
Rhinitis (%), n=349	142 (94.0)	75 (91.5)	37 (84.1)	49 (83.1)	10 (76.9)	313 (89.7)	**0.028**
Glue ear (%), n=333	93 (64.1)	45 (58.4)	34 (81.0)	32 (57.1)	8 (61.5)	214 (63.7)	0.099
Situs solitus (%), n=380	69 (42.9)	36 (39.1)	48 (100)	40 (60.6)	13 (100)	206 (54.2)	**<0.001**

N-DRC = nexin-dynein regulatory complex; SD = standard deviation; IQR = interquartile range; + # difference between groups was statistically significant (ANOVA followed by Tukey for pairwise comparisons).

References

1. Lucas JS, Barbato A, Collins SA, Goutaki M, Behan L, Caudri D, Dell S, Eber E, Escudier E, Hirst RA, Hogg C, Jorissen M, Latzin P, Legendre M, Leigh MW, Midulla F, Nielsen KG, Omran H, Papon J-F, Pohunek P, Redfern B, Rigau D, Rindlisbacher B, Santamaria F, Shoemark A, Snijders D, Tonia T, Titieni A, Walker WT, Werner C, Bush A, Kuehni CE. European Respiratory Society guidelines for the diagnosis of primary ciliary dyskinesia. *European Respiratory Journal* 2017: 49(1): 1601090.
2. Richards S, Aziz N, Bale S, Bick D, Das S, Gastier-Foster J, Grody WW, Hegde M, Lyon E, Spector E, Voelkerding K, Rehm HL. Standards and guidelines for the interpretation of sequence variants: a joint consensus recommendation of the American College of Medical Genetics and Genomics and the Association for Molecular Pathology. *Genet Med* 2015: 17(5): 405-424.
3. Carlsson G. Topology and data. *Bull Amer Math Soc* 2009: 46(2): 255-308.
4. Glushakov S, Kotenko, I., Rekalo, A. Handling Missing Data in Clinical Trials Using Topological Data Analysis. PhUSE EU Connect 2018 (https://www.lexjansen.com/phuse/2018/ml/ML07.pdf).
5. Best S, Shoemark A, Rubbo B, Patel MP, Fassad MR, Dixon M, Rogers AV, Hirst RA, Rutman A, Ollosson S, Jackson CL, Goggin P, Thomas S, Pengelly R, Cullup T, Pissaridou E, Hayward J, Onoufriadis A, O'Callaghan C, Loebinger MR, Wilson R, Chung EM, Kenia P, Doughty VL, Carvalho JS, Lucas JS, Mitchison HM, Hogg C. Risk factors for situs defects and congenital heart disease in primary ciliary dyskinesia. *Thorax* 2019: 74(2): 203-205.
6. Omoyinmi E, Standing A, Keylock A, Price-Kuehne F, Melo Gomes S, Rowczenio D, Nanthapisal S, Cullup T, Nyanhete R, Ashton E, Murphy C, Clarke M, Ahlfors H, Jenkins L, Gilmour K, Eleftheriou D, Lachmann HJ, Hawkins PN, Klein N, Brogan PA. Clinical impact of a targeted next-generation sequencing gene panel for autoinflammation and vasculitis. *PloS one* 2017: 12(7): e0181874.
7. Quanjer PH, Stanojevic S, Cole TJ, Baur X, Hall GL, Culver BH, Enright PL, Hankinson JL, Ip MS, Zheng J, Stocks J, Initiative ERSGLF. Multi-ethnic reference values for spirometry for the 3-95-yr age range: the global lung function 2012 equations. *Eur Respir J* 2012: 40(6): 1324-1343.
8. Group WHOMGRS. WHO Child Growth Standards based on length/height, weight and age. *Acta paediatrica* 2006: 450: 76-85.
9. Hjeij R, Lindstrand A, Francis R, Zariwala MA, Liu X, Li Y, Damerla R, Dougherty GW, Abouhamed M, Olbrich H, Loges NT, Pennekamp P, Davis EE, Carvalho CM, Pehlivan D, Werner C, Raidt J, Kohler G, Haffner K, Reyes-Mugica M, Lupski JR, Leigh MW, Rosenfeld M, Morgan LC, Knowles MR, Lo CW, Katsanis N, Omran H. ARMC4 mutations cause primary ciliary dyskinesia with randomization of left/right body asymmetry. *Am J Hum Genet* 2013: 93(2): 357-367.
10. Onoufriadis A, Shoemark A, Munye MM, James CT, Schmidts M, Patel M, Rosser EM, Bacchelli C, Beales PL, Scambler PJ, Hart SL, Danke-Roelse JE, Sloper JJ, Hull S, Hogg C, Emes RD, Pals G, Moore AT, Chung EM, Uk10K, Mitchison HM. Combined exome and whole-genome sequencing identifies mutations in ARMC4 as a cause of primary ciliary dyskinesia with defects in the outer dynein arm. *J Med Genet* 2014: 51(1): 61-67.
11. Panizzi JR, Becker-Heck A, Castleman VH, Al-Mutairi DA, Liu Y, Loges NT, Pathak N, Austin-Tse C, Sheridan E, Schmidts M, Olbrich H, Werner C, Haffner K, Hellman N, Chodhari R, Gupta A, Kramer-Zucker A, Olale F, Burdine RD, Schier AF, O'Callaghan C, Chung EM, Reinhardt R, Mitchison HM, King SM, Omran H, Drummond IA. CCDC103 mutations cause primary ciliary dyskinesia by disrupting assembly of ciliary dynein arms. *Nat Genet* 2012: 44(6): 714-719.
12. Casey JP, McGettigan PA, Healy F, Hogg C, Reynolds A, Kennedy BN, Ennis S, Slattery D, Lynch SA. Unexpected genetic heterogeneity for primary ciliary dyskinesia in the Irish Traveller population. *Eur J Hum Genet* 2015: 23(2): 210-217.
13. D'Andrea G, Schiavulli M, Dimatteo C, Santacroce R, Guerra E, Longo VA, Grandone E, Margaglione M. Homozygosity by descent of a 3Mb chromosome 17 haplotype causes coinheritance of Glanzmann thrombasthenia and primary ciliary dyskinesia. *Blood* 2013: 122(26): 4289-4291.
14. Onoufriadis A, Paff T, Antony D, Shoemark A, Micha D, Kuyt B, Schmidts M, Petridi S, Dankert-Roelse JE, Haarman EG, Daniels JM, Emes RD, Wilson R, Hogg C, Scambler PJ, Chung EM, Uk10K, Pals G, Mitchison HM. Splice-site mutations in the axonemal outer dynein arm docking complex gene CCDC114 cause primary ciliary dyskinesia. *Am J Hum Genet* 2013: 92(1): 88-98.
15. Antony D, Becker-Heck A, Zariwala MA, Schmidts M, Onoufriadis A, Forouhan M, Wilson R, Taylor-Cox T, Dewar A, Jackson C, Goggin P, Loges NT, Olbrich H, Jaspers M, Jorissen M, Leigh MW, Wolf WE, Daniels ML, Noone PG, Ferkol TW, Sagel SD, Rosenfeld M, Rutman A, Dixit A, O'Callaghan C, Lucas JS, Hogg C, Scambler PJ, Emes RD, Uk10k, Chung EM, Shoemark A, Knowles MR, Omran H, Mitchison HM. Mutations in CCDC39 and CCDC40 are the major cause of primary ciliary dyskinesia with axonemal disorganization and absent inner dynein arms. *Hum Mutat* 2013: 34(3): 462-472.

16. Merveille AC, Davis EE, Becker-Heck A, Legendre M, Amirav I, Bataille G, Belmont J, Beydon N, Billen F, Clement A, Clercx C, Coste A, Crosbie R, de Blic J, Deleuze S, Duquesnoy P, Escalier D, Escudier E, Fliegauf M, Horvath J, Hill K, Jorissen M, Just J, Kispert A, Lathrop M, Loges NT, Marthin JK, Momozawa Y, Montantin G, Nielsen KG, Olbrich H, Papon JF, Rayet I, Roger G, Schmidts M, Tenreiro H, Towbin JA, Zelenika D, Zentgraf H, Georges M, Lequarre AS, Katsanis N, Omran H, Amselem S. CCDC39 is required for assembly of inner dynein arms and the dynein regulatory complex and for normal ciliary motility in humans and dogs. *Nat Genet* 2011: 43(1): 72-78.
17. Blanchon S, Legendre M, Copin B, Duquesnoy P, Montantin G, Kott E, Dastot F, Jeanson L, Cachanado M, Rousseau A, Papon JF, Beydon N, Brouard J, Crestani B, Deschildre A, Desir J, Dollfus H, Leheup B, Tamalet A, Thumerelle C, Vojtek AM, Escalier D, Coste A, de Blic J, Clement A, Escudier E, Amselem S. Delineation of CCDC39/CCDC40 mutation spectrum and associated phenotypes in primary ciliary dyskinesia. *J Med Genet* 2012: 49(6): 410-416.
18. Kim RH, D AH, Cutz E, Knowles MR, Nelligan KA, Nykamp K, Zariwala MA, Dell SD. The role of molecular genetic analysis in the diagnosis of primary ciliary dyskinesia. *Annals of the American Thoracic Society* 2014: 11(3): 351-359.
19. Becker-Heck A, Zohn IE, Okabe N, Pollock A, Lenhart KB, Sullivan-Brown J, McSheene J, Loges NT, Olbrich H, Haeffner K, Fliegauf M, Horvath J, Reinhardt R, Nielsen KG, Marthin JK, Baktai G, Anderson KV, Geisler R, Niswander L, Omran H, Burdine RD. The coiled-coil domain containing protein CCDC40 is essential for motile cilia function and left-right axis formation. *Nat Genet* 2011: 43(1): 79-84.
20. Zariwala MA, Gee HY, Kurkowiak M, Al-Mutairi DA, Leigh MW, Hurd TW, Hjeij R, Dell SD, Chaki M, Dougherty GW, Adan M, Spear PC, Esteve-Rudd J, Loges NT, Rosenfeld M, Diaz KA, Olbrich H, Wolf WE, Sheridan E, Batten TF, Halbritter J, Porath JD, Kohl S, Lovric S, Hwang DY, Pittman JE, Burns KA, Ferkol TW, Sagel SD, Olivier KN, Morgan LC, Werner C, Raidt J, Pennekamp P, Sun Z, Zhou W, Airik R, Natarajan S, Allen SJ, Amirav I, Wieczorek D, Landwehr K, Nielsen K, Schwerk N, Sertic J, Kohler G, Washburn J, Levy S, Fan S, Koerner-Rettberg C, Amselem S, Williams DS, Mitchell BJ, Drummond IA, Otto EA, Omran H, Knowles MR, Hildebrandt F. ZMYND10 is mutated in primary ciliary dyskinesia and interacts with LRRC6. *Am J Hum Genet* 2013: 93(2): 336-345.
21. Austin-Tse C, Halbritter J, Zariwala MA, Gilberti RM, Gee HY, Hellman N, Pathak N, Liu Y, Panizzi JR, Patel-King RS, Tritschler D, Bower R, O'Toole E, Porath JD, Hurd TW, Chaki M, Diaz KA, Kohl S, Lovric S, Hwang DY, Braun DA, Schueler M, Airik R, Otto EA, Leigh MW, Noone PG, Carson JL, Davis SD, Pittman JE, Ferkol TW, Atkinson JJ, Olivier KN, Sagel SD, Dell SD, Rosenfeld M, Milla CE, Loges NT, Omran H, Porter ME, King SM, Knowles MR, Drummond IA, Hildebrandt F. Zebrafish Ciliopathy Screen Plus Human Mutational Analysis Identifies C21orf59 and CCDC65 Defects as Causing Primary Ciliary Dyskinesia. *Am J Hum Genet* 2013: 93(4): 672-686.
22. Wallmeier J, Al-Mutairi DA, Chen CT, Loges NT, Pennekamp P, Menchen T, Ma L, Shamseldin HE, Olbrich H, Dougherty GW, Werner C, Alsabah BH, Kohler G, Jaspers M, Boon M, Griese M, Schmitt-Grohe S, Zimmermann T, Koerner-Rettberg C, Horak E, Kintner C, Alkuraya FS, Omran H. Mutations in CCNO result in congenital mucociliary clearance disorder with reduced generation of multiple motile cilia. *Nat Genet* 2014: 46(6): 646-651.
23. Watson CM, Crinnion LA, Morgan JE, Harrison SM, Diggle CP, Adlard J, Lindsay HA, Camm N, Charlton R, Sheridan E, Bonthron DT, Taylor GR, Carr IM. Robust diagnostic genetic testing using solution capture enrichment and a novel variant-filtering interface. *Hum Mutat* 2014: 35(4): 434-441.
24. Mitchison HM, Schmidts M, Loges NT, Freshour J, Dritsoula A, Hirst RA, O'Callaghan C, Blau H, Al Dabbagh M, Olbrich H, Beales PL, Yagi T, Mussaffi H, Chung EM, Omran H, Mitchell DR. Mutations in axonemal dynein assembly factor DNAAF3 cause primary ciliary dyskinesia. *Nat Genet* 2012: 44(4): 381-389, S381-382.
25. Tarkar A, Loges NT, Slagle CE, Francis R, Dougherty GW, Tamayo JV, Shook B, Cantino M, Schwartz D, Jahnke C, Olbrich H, Werner C, Raidt J, Pennekamp P, Abouhamed M, Hjeij R, Kohler G, Griese M, Li Y, Lemke K, Klena N, Liu X, Gabriel G, Tobita K, Jaspers M, Morgan LC, Shapiro AJ, Letteboer SJ, Mans DA, Carson JL, Leigh MW, Wolf WE, Chen S, Lucas JS, Onoufriadis A, Plagnol V, Schmidts M, Boldt K, Uk10K, Roepman R, Zariwala MA, Lo CW, Mitchison HM, Knowles MR, Burdine RD, Loturco JJ, Omran H. DYX1C1 is required for axonemal dynein assembly and ciliary motility. *Nat Genet* 2013: 45(9): 995-1003.
26. Knowles MR, Leigh MW, Carson JL, Davis SD, Dell SD, Ferkol TW, Olivier KN, Sagel SD, Rosenfeld M, Burns KA, Minnix SL, Armstrong MC, Lori A, Hazucha MJ, Loges NT, Olbrich H, Becker-Heck A, Schmidts M, Werner C, Omran H, Zariwala MA, Genetic Disorders of Mucociliary Clearance C. Mutations of DNAH11 in patients with primary ciliary dyskinesia with normal ciliary ultrastructure. *Thorax* 2012: 67(5): 433-441.
27. Shoemark A, Burgoyne T, Kwan R, Dixon M, Patel MP, Rogers AV, Onoufriadis A, Scully J, Daudvohra F, Cullup T, Loebinger MR, Wilson R, Chung EMK, Bush A, Mitchison HM, Hogg C. Primary ciliary dyskinesia with normal ultrastructure: three-dimensional tomography detects absence of DNAH11. *Eur Respir J* 2018: 51(2).
28. Lucas JS, Adam EC, Goggin PM, Jackson CL, Powles-Glover N, Patel SH, Humphreys J, Fray MD, Falconnet E, Blouin JL, Cheeseman MT, Bartoloni L, Norris DP, Lackie PM. Static respiratory cilia associated with mutations in Dnahc11/DNAH11: a mouse model of PCD. *Hum Mutat* 2012: 33(3): 495-503.

29. Hornef N, Olbrich H, Horvath J, Zariwala MA, Fliegauf M, Loges NT, Wildhaber J, Noone PG, Kennedy M, Antonarakis SE, Blouin JL, Bartoloni L, Nusslein T, Ahrens P, Griese M, Kuhl H, Sudbrak R, Knowles MR, Reinhardt R, Omran H. DNAH5 mutations are a common cause of primary ciliary dyskinesia with outer dynein arm defects. *American journal of respiratory and critical care medicine* 2006: 174(2): 120-126.
30. Berg JS, Evans JP, Leigh MW, Omran H, Bizon C, Mane K, Knowles MR, Weck KE, Zariwala MA. Next generation massively parallel sequencing of targeted exomes to identify genetic mutations in primary ciliary dyskinesia: implications for application to clinical testing. *Genet Med* 2011: 13(3): 218-229.
31. Djakow J, Kramna L, Dusatkova L, Uhlik J, Pursiheimo JP, Svobodova T, Pohunek P, Cinek O. An effective combination of sanger and next generation sequencing in diagnostics of primary ciliary dyskinesia. *Pediatric pulmonology* 2016: 51(5): 498-509.
32. Olbrich H, Haffner K, Kispert A, Volkel A, Volz A, Sasmaz G, Reinhardt R, Hennig S, Lehrach H, Konietzko N, Zariwala M, Noone PG, Knowles M, Mitchison HM, Meeks M, Chung EM, Hildebrandt F, Sudbrak R, Omran H. Mutations in DNAH5 cause primary ciliary dyskinesia and randomization of left-right asymmetry. *Nat Genet* 2002: 30(2): 143-144.
33. Failly M, Bartoloni L, Letourneau A, Munoz A, Falconnet E, Rossier C, de Santi MM, Santamaria F, Sacco O, DeLozier-Blanchet CD, Lazor R, Blouin JL. Mutations in DNAH5 account for only 15% of a non-preselected cohort of patients with primary ciliary dyskinesia. *J Med Genet* 2009: 46(4): 281-286.
34. Raidt J, Wallmeier J, Hjeij R, Onnebrink JG, Pennekamp P, Loges NT, Olbrich H, Haffner K, Dougherty GW, Omran H, Werner C. Ciliary beat pattern and frequency in genetic variants of primary ciliary dyskinesia. *Eur Respir J* 2014: 44(6): 1579-1588.
35. Knowles MR, Leigh MW, Ostrowski LE, Huang L, Carson JL, Hazucha MJ, Yin W, Berg JS, Davis SD, Dell SD, Ferkol TW, Rosenfeld M, Sagel SD, Milla CE, Olivier KN, Turner EH, Lewis AP, Bamshad MJ, Nickerson DA, Shendure J, Zariwala MA, Genetic Disorders of Mucociliary Clearance C. Exome sequencing identifies mutations in CCDC114 as a cause of primary ciliary dyskinesia. *Am J Hum Genet* 2013: 92(1): 99-106.
36. Xiong HY, Alipanahi B, Lee LJ, Bretschneider H, Merico D, Yuen RK, Hua Y, Gueroussov S, Najafabadi HS, Hughes TR, Morris Q, Barash Y, Krainer AR, Jojic N, Scherer SW, Blencowe BJ, Frey BJ. RNA splicing. The human splicing code reveals new insights into the genetic determinants of disease. *Science* 2015: 347(6218): 1254806.
37. Boaretto F, Snijders D, Salvoro C, Spalletta A, Mostacciuolo ML, Collura M, Cazzato S, Girosi D, Silvestri M, Rossi GA, Barbato A, Vazza G. Diagnosis of Primary Ciliary Dyskinesia by a Targeted Next-Generation Sequencing Panel: Molecular and Clinical Findings in Italian Patients. *The Journal of molecular diagnostics : JMD* 2016: 18(6): 912-922.
38. Zariwala MA, Leigh MW, Ceppa F, Kennedy MP, Noone PG, Carson JL, Hazucha MJ, Lori A, Horvath J, Olbrich H, Loges NT, Bridoux AM, Pennarun G, Duriez B, Escudier E, Mitchison HM, Chodhari R, Chung EM, Morgan LC, de Iongh RU, Rutland J, Pradal U, Omran H, Amselem S, Knowles MR. Mutations of DNAI1 in primary ciliary dyskinesia: evidence of founder effect in a common mutation. *American journal of respiratory and critical care medicine* 2006: 174(8): 858-866.
39. Wirschell M, Olbrich H, Werner C, Tritschler D, Bower R, Sale WS, Loges NT, Pennekamp P, Lindberg S, Stenram U, Carlen B, Horak E, Kohler G, Nurnberg P, Nurnberg G, Porter ME, Omran H. The nexin-dynein regulatory complex subunit DRC1 is essential for motile cilia function in algae and humans. *Nat Genet* 2013: 45(3): 262-268.
40. Olcese C, Patel MP, Shoemark A, Kiviluoto S, Legendre M, Williams HJ, Vaughan CK, Hayward J, Goldenberg A, Emes RD, Munye MM, Dyer L, Cahill T, Bevillard J, Gehrig C, Guipponi M, Chantot S, Duquesnoy P, Thomas L, Jeanson L, Copin B, Tamalet A, Thauvin-Robinet C, Papon JF, Garin A, Pin I, Vera G, Aurora P, Fassad MR, Jenkins L, Boustred C, Cullup T, Dixon M, Onoufriadis A, Bush A, Chung EM, Antonarakis SE, Loebinger MR, Wilson R, Armengot M, Escudier E, Hogg C, Group UKR, Amselem S, Sun Z, Bartoloni L, Blouin JL, Mitchison HM. X-linked primary ciliary dyskinesia due to mutations in the cytoplasmic axonemal dynein assembly factor PIH1D3. *Nature communications* 2017: 8: 14279.
41. Kott E, Legendre M, Copin B, Papon JF, Dastot-Le Moal F, Montantin G, Duquesnoy P, Piterboth W, Amram D, Bassinet L, Beucher J, Beydon N, Deneuville E, Houdouin V, Journel H, Just J, Nathan N, Tamalet A, Collot N, Jeanson L, Le Gouez M, Vallette B, Vojtek AM, Epaud R, Coste A, Clement A, Housset B, Louis B, Escudier E, Amselem S. Loss-of-function mutations in RSPH1 cause primary ciliary dyskinesia with central-complex and radial-spoke defects. *Am J Hum Genet* 2013: 93(3): 561-570.
42. Daniels ML, Leigh MW, Davis SD, Armstrong MC, Carson JL, Hazucha M, Dell SD, Eriksson M, Collins FS, Knowles MR, Zariwala MA. Founder mutation in RSPH4A identified in patients of Hispanic descent with primary ciliary dyskinesia. *Hum Mutat* 2013: 34(10): 1352-1356.
43. Castleman VH, Romio L, Chodhari R, Hirst RA, de Castro SC, Parker KA, Ybot-Gonzalez P, Emes RD, Wilson SW, Wallis C, Johnson CA, Herrera RJ, Rutman A, Dixon M, Shoemark A, Bush A, Hogg C, Gardiner RM, Reish O, Greene ND, O'Callaghan C, Purton S, Chung EM, Mitchison HM. Mutations in radial spoke head protein genes RSPH9 and

RSPH4A cause primary ciliary dyskinesia with central-microtubular-pair abnormalities. *Am J Hum Genet* 2009: 84(2): 197-209.
44. Marshall CR, Scherer SW, Zariwala MA, Lau L, Paton TA, Stockley T, Jobling RK, Ray PN, Knowles MR, Hall DA, Dell SD, Kim RH. Whole-Exome Sequencing and Targeted Copy Number Analysis in Primary Ciliary Dyskinesia. *G3 (Bethesda, Md)* 2015: 5(8): 1775-1781.
45. Moore DJ, Onoufriadis A, Shoemark A, Simpson MA, zur Lage PI, de Castro SC, Bartoloni L, Gallone G, Petridi S, Woollard WJ, Antony D, Schmidts M, Didonna T, Makrythanasis P, Bevillard J, Mongan NP, Djakow J, Pals G, Lucas JS, Marthin JK, Nielsen KG, Santoni F, Guipponi M, Hogg C, Antonarakis SE, Emes RD, Chung EM, Greene ND, Blouin JL, Jarman AP, Mitchison HM. Mutations in ZMYND10, a gene essential for proper axonemal assembly of inner and outer dynein arms in humans and flies, cause primary ciliary dyskinesia. *Am J Hum Genet* 2013: 93(2): 346-356.